

## CHAPTER 3

---

# NOZZLE THEORY AND THERMODYNAMIC RELATIONS

---

Thermodynamic relations of the processes inside a rocket nozzle and chamber furnish the mathematical tools needed to calculate the performance and determine several of the key design parameters of rocket propulsion systems. They are useful as a means of evaluating and comparing the performance of various rocket systems; they permit the prediction of the operating performance of any rocket unit that uses the thermodynamic expansion of a gas, and the determination of several necessary design parameters, such as nozzle size and generic shape, for any given performance requirement. This theory applies to chemical rocket propulsion systems (both liquid and solid propellant types), nuclear rockets, solar heated and resistance or arc heated electrical rocket systems, and to any propulsion system that uses the expansion of a gas as the propulsive mechanism for ejecting matter at high velocity.

These thermodynamic relations, which are fundamental and important in analysis and design of rocket units, are introduced and explained in this chapter. The utilization of these equations should give the reader a basic understanding of the thermodynamic processes involved in rocket gas behavior and expansion. A knowledge of elementary thermodynamics and fluid mechanics on the part of the reader is assumed (see Refs. 1-1, 3-1, 3-2, and 3-3). This chapter also addresses different nozzle configurations, non-optimum performance, energy losses, nozzle alignment, variable thrust and four different ways for establishing nozzle performance parameters.

### 3.1. IDEAL ROCKET

The concept of ideal rocket propulsion systems is useful because the relevant basic thermodynamic principles can be expressed as simple mathematical relationships, which are given in subsequent sections of this chapter. These equations theoretically describe a quasi-one-dimensional nozzle flow, which corresponds to an idealization and simplification of the full two- or three-dimensional equations and the real aerothermochemical behavior. However, with the assumptions and simplifications stated below, they are very adequate for obtaining useful solutions to many rocket propulsion systems. For chemical rocket propulsion the measured actual performance is usually between 1 and 6% below the calculated ideal value. In designing new rockets, it has become accepted practice to use ideal rocket parameters which can then be modified by appropriate corrections, such as those discussed in Section 5 of this chapter. An *ideal rocket* unit is one for which the following assumptions are valid:

1. The working substance (or chemical reaction products) is *homogeneous*.
2. All the species of the working fluid are *gaseous*. Any condensed phases (liquid or solid) add a negligible amount to the total mass.
3. The working substance obeys the *perfect gas law*.
4. There is no *heat transfer* across the rocket walls; therefore, the flow is *adiabatic*.
5. There is no appreciable *friction* and all *boundary layer* effects are neglected.
6. There are no *shock waves* or *discontinuities* in the nozzle flow.
7. The *propellant flow* is *steady* and *constant*. The expansion of the working fluid is uniform and steady, without vibration. Transient effects (i.e., start up and shut down) are of very short duration and may be neglected.
8. All exhaust gases leaving the rocket have an *axially directed velocity*.
9. The gas velocity, pressure, temperature, and density are all uniform across any section normal to the nozzle axis.
10. *Chemical equilibrium* is established within the rocket chamber and the gas composition does not change in the nozzle (frozen flow).
11. Stored propellants are at room temperature. Cryogenic propellants are at their boiling points.

These assumptions permit the derivation of a simple, quasi-one-dimensional theory as developed in subsequent sections. Later in this book we present more sophisticated theories or introduce correction factors for several of the items on the list, and they allow a more accurate determination of the simplified analysis. The next paragraph explains why these assumptions cause only small errors.

For a liquid propellant rocket the idealized theory postulates an injection system in which the fuel and oxidizer are mixed perfectly so that a homogeneous working substance results. A good rocket injector can approach this condition closely. For a solid propellant rocket unit, the propellant must essentially be homogeneous and uniform and the burning rate must be steady. For nuclear, solar-heated or arc-heated rockets, it is assumed that the hot gases are uniform in temperature at any cross-section and steady in flow. Because chamber temperatures are typically high (2500 to 3600 K for common propellants), all gases are well above their respective saturation conditions and actually follow the perfect gas law very closely. Postulates 4, 5, and 6 above allow the use of the *isentropic expansion* relations in the rocket nozzle, thereby describing the maximum conversion of heat to kinetic energy of the jet. This also implies that the nozzle flow is thermodynamically reversible. Wall friction losses are difficult to determine accurately but they are usually small in nozzles. Except for very small chambers, the energy lost as heat to the walls of the rocket is usually less than 1% (occasionally up to 2%) of the total energy and can therefore be neglected. Short-term fluctuations of the steady propellant flow rate and pressure are usually less than 5% of the rated value, their effect on rocket performance is small and can be neglected. In well-designed supersonic nozzles, the conversion of thermal energy into directed kinetic energy of the exhaust gases proceeds smoothly and without normal shocks or discontinuities; thus the flow expansion losses are generally small.

Some companies and some authors do not include all or the same eleven items listed above in their definition of an ideal rocket. For example, instead of assumption 8 (all nozzle exit velocity is axially directed), some use a conical exit nozzle with a  $15^\circ$  half-angle as their base configuration in their ideal nozzle; this discounts the divergence losses, which are described later in this chapter.

### 3.2. SUMMARY OF THERMODYNAMIC RELATIONS

In this section we review briefly some of the basic relationships needed for the development of the nozzle flow equations. Rigorous derivations and discussions of these relations can be found in many thermodynamics or fluid dynamics texts, such as Refs. 3-1 and 3-2.

The principle of *conservation of energy* can be readily applied to the adiabatic, no shaft-work process inside the nozzle. Furthermore, without shocks or friction, the flow entropy change is zero. The concept of *enthalpy* is useful in flow systems; the enthalpy comprises the *internal thermal energy* plus the *flow work* (or work performed by the gas at a velocity  $v$  in crossing a boundary). For ideal gases the enthalpy can conveniently be expressed as the product of the specific heat  $c_p$  times the absolute temperature  $T$  (the specific heat at constant pressure is formally defined as the partial derivative of the enthalpy with respect to temperature at constant pressure). Under the above assumptions, the total or stagnation enthalpy per unit mass  $h_0$  is constant, i.e.,

$$h_0 = h + v^2/2J = \text{constant} \quad (3-1)$$

In the above,  $J$  is the mechanical equivalent of heat which is inserted only when thermal units (i.e., the Btu and calorie) are mixed with mechanical units (i.e., the ft-lbf and the joule). In SI units (kg, m, sec) the value of  $J$  is one. In the English Engineering system of units another constant (see Appendix 1) has to be provided to account for the mass units (i.e., the lbm). The conservation of energy for isentropic flow between any two sections  $x$  and  $y$  shows that the decrease in enthalpy or thermal content of the flow appears as an increase of kinetic energy since and any changes in potential energy may be neglected.

$$h_x - h_y = \frac{1}{2}(v_y^2 - v_x^2)/J = c_p(T_x - T_y) \quad (3-2)$$

The principle of *conservatism of mass* in a steady flow with a single inlet and single outlet is expressed by equating the mass flow rate  $\dot{m}$  at any section  $x$  to that at any other section  $y$ ; this is known in mathematical form as the continuity equation. Written in terms of the cross-sectional area  $A$ , the velocity  $v$ , and the specific volume  $V$ ,

$$\dot{m}_x = \dot{m}_y \equiv \dot{m} = Av/V \quad (3-3)$$

The *perfect gas law* is written as

$$p_x V_x = RT_x \quad (3-4)$$

where the gas constant  $R$  is found from the universal gas constant  $R'$  divided by the molecular mass  $\mathfrak{M}$  of the flowing gas mixture. The molecular volume at standard conditions becomes  $22.41 \text{ m}^3/\text{kg-mol}$  or  $\text{ft}^3/\text{lb-mol}$  and it relates to a value of  $R' = 8314.3 \text{ J/kg-mole-K}$  or  $1544 \text{ ft-lbf/lb-mole-R}$ . One often finds Eq. 3-3 written in terms of density  $\rho$  which is the reciprocal of the specific volume  $V$ . The specific heat at constant pressure  $c_p$ , the specific heat at constant volume  $c_v$ , and their ratio  $k$  are constant for perfect gases over a wide range of temperatures and are related.

$$k = c_p/c_v \quad (3-5a)$$

$$c_p - c_v = R/J \quad (3-5b)$$

$$c_p = kR/(k-1)J \quad (3-6)$$

For an *isentropic flow process* the following relations hold between any points  $x$  and  $y$ :

$$T_x/T_y = (p_x/p_y)^{(k-1)/k} = (V_y/V_x)^{k-1} \quad (3-7)$$

During an isentropic nozzle expansion the pressure drops substantially, the absolute temperature drops somewhat less, and the specific volume increases. When a flow is stopped isentropically the prevailing conditions are known as *stagnation conditions* and are designated by the subscript “0”. Sometimes the word “total” is used instead of stagnation. As can be seen from Eq. 3-1 the stagnation enthalpy consists of the sum of the static or local enthalpy and the fluid kinetic energy. The stagnation temperature  $T_0$  is found from the energy equation as

$$T_0 = T + v^2/(2c_p J) \quad (3-8)$$

where  $T$  is the absolute fluid static temperature. In adiabatic flows, the stagnation temperature remains constant. The relationship of the stagnation pressure to the local pressure in the flow can be found from the previous two equations:

$$p_0/p = [1 + v^2/(2c_p J T)]^{k/(k-1)} = (V/V_0)^k \quad (3-9)$$

When the local velocity comes close to zero, the local temperature and pressure will approach the stagnation pressure and stagnation temperature. In a combustion chamber, where the gas velocity is small, the local combustion pressure is essentially equal to the stagnation pressure. The *velocity of sound*  $a$  or the acoustic velocity in ideal gases is independent of pressure. It is defined as

$$a = \sqrt{kRT} \quad (3-10)$$

In the English Engineering (EE) system the value of  $R$  has to be corrected and the constant  $g_0$  is added. Equation 3-10 becomes  $\sqrt{g_0 kRT}$ . This correction factor must be applied wherever  $R$  is used in EE units. The *Mach number*  $M$  is a dimensionless flow parameter and is used to define the ratio of the flow velocity  $v$  to the local acoustic velocity  $a$ .

$$M = v/a = v/\sqrt{kRT} \quad (3-11)$$

A Mach number less than one corresponds to subsonic flow and greater than one to supersonic flow. When the Mach number is equal to one then the flow is moving at precisely the velocity of sound. It is shown later that at the throat of all supersonic nozzles the Mach number must be equal to one. The relation between stagnation temperature and Mach number can now be written from Eqs. 3-2, 3-7, and 3-10 as

$$T_0 = T \left[ 1 + \frac{1}{2}(k-1)M^2 \right] \quad (3-12)$$

or

$$M = \sqrt{\frac{2}{k-1} \left( \frac{T_0}{T} - 1 \right)}$$

$T_0$  and  $p_0$  designate the stagnation values of the temperature and pressure. Unlike the temperature, the stagnation pressure during an adiabatic nozzle expansion remains constant only for isentropic flows. It can be computed from

$$p_0 = p \left[ 1 + \frac{1}{2}(k-1)M^2 \right]^{k/(k-1)} \quad (3-13)$$

The *area ratio* for a nozzle with isentropic flow can be expressed in terms of Mach numbers for any points  $x$  and  $y$  within the nozzle. This relationship, along with those for the ratios  $T/T_0$  and  $p/p_0$ , is plotted in Fig. 3-1 for  $A_x = A_t$  and  $M_x = 1.0$ . Otherwise,

$$\frac{A_y}{A_x} = \frac{M_x}{M_y} \sqrt{\frac{\left\{ 1 + [(k-1)/2]M_y^2 \right\}^{(k+1)/(k-1)}}{\left\{ 1 + [(k-1)/2]M_x^2 \right\}}} \quad (3-14)$$

As can be seen from Fig. 3-1, for subsonic flow the chamber contraction ratio  $A_1/A_t$  can be small, with values of 3 to 6, and the passage is convergent. There is no noticeable effect from variations of  $k$ . In solid rocket motors the chamber area  $A_1$  refers to the flow passage or port cavity in the virgin grain. With supersonic flow the nozzle section diverges and the area ratio becomes large very quickly; the area ratio is significantly influenced by the value of  $k$ . The area ratio  $A_2/A_t$  ranges between 15 and 30 at  $M = 4$ , depending on the value of  $k$ . On the other hand, pressure ratios depend little on  $k$  whereas temperature ratios show more variation.

The average *molecular mass*  $\mathfrak{M}$  of a mixture of gases is the sum of all the molar fractions  $n_i$  multiplied by the molecular mass of each chemical species ( $n_i\mathfrak{M}_i$ ) and then divided by the sum of all molar mass fractions. This is further elaborated upon in Chapter 5. The symbol  $\mathfrak{M}$  is used to avoid confusion with  $M$  for the Mach number. In many pieces of rocket literature  $\mathfrak{M}$  is called molecular weight.

**Example 3-1.** An ideal rocket chamber is to operate at sea level using propellants whose combustion products have a specific heat ratio  $k$  of 1.30. Determine the required chamber pressure and nozzle area ratio between throat and exit if the nozzle exit Mach number is 2.40. The nozzle inlet Mach number may be considered to be negligibly small.

**SOLUTION.** For optimum expansion the nozzle exit pressure should be equal to the atmospheric pressure which has the value 0.1013 MPa. If the chamber velocity is small, the chamber pressure is equal to the total or stagnation pressure, which is, from Eq. 3-13,

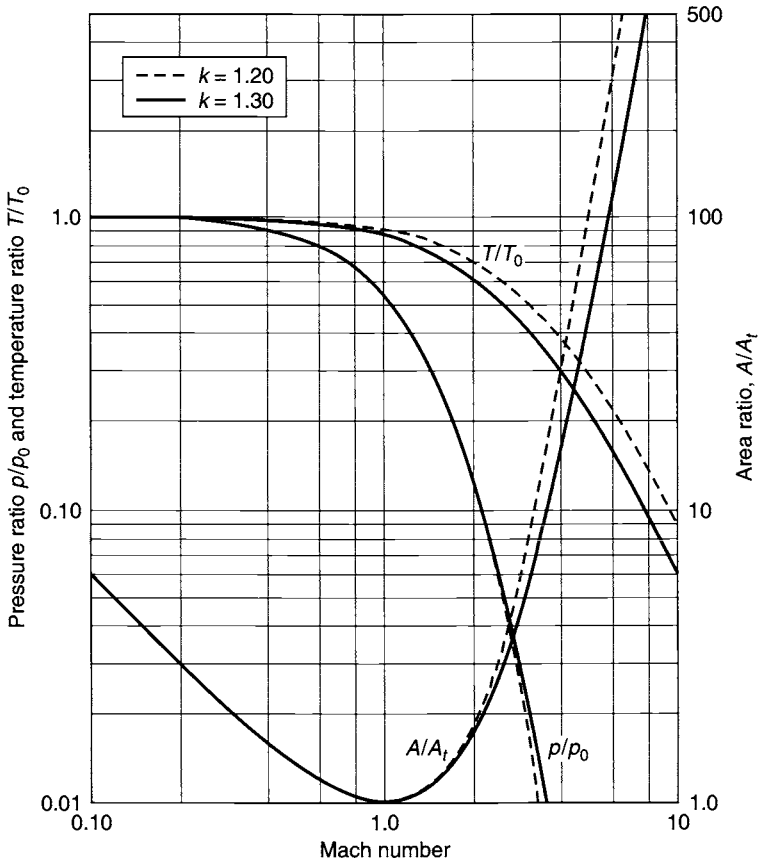


**FIGURE 3-1.** Relationship of area ratio, pressure ratio, and temperature ratio as functions of Mach number in a De Laval nozzle for the subsonic and supersonic nozzle regions.

$$\begin{aligned}
 p_0 &= p \left[ 1 + \frac{1}{2}(k-1)M^2 \right]^{k/(k-1)} \\
 &= 0.1013 \left[ 1 + \frac{1}{2} \times 0.30 \times 2.40^2 \right]^{1.3/0.3} = 1.51 \text{ MPa}
 \end{aligned}$$

The nozzle area is determined from Eq. 3-14 by setting  $M_t = 1.0$  at the throat (see also Fig. 3-1):

$$\frac{A_2}{A_t} = \frac{1.0}{2.40} \sqrt{\left( \frac{1 + 0.15 \times 2.4^2}{1 + 0.15} \right)^{2.3/0.3}} = 2.64$$

### 3.3. ISENTROPIC FLOW THROUGH NOZZLES

In a converging-diverging nozzle a large fraction of the thermal energy of the gases in the chamber is converted into kinetic energy. As will be explained, the gas pressure and temperature drop dramatically and the gas velocity can reach values in excess of two miles per second. This is a reversible, essentially isentropic flow process and its analysis is described here. If a nozzle inner wall has a flow obstruction or a wall protrusion (a piece of weld splatter or slag), then the kinetic gas energy is locally converted back into thermal energy essentially equal to the stagnation temperature and stagnation pressure in the chamber. Since this would lead quickly to a local overheating and failure of the wall, nozzle inner walls have to be smooth without any protrusion. Stagnation conditions can also occur at the leading edge of a jet vane (described in Chapter 16) or at the tip of a gas sampling tube inserted into the flow.

#### Velocity

From Eq. 3-2 the nozzle exit velocity  $v_2$  can be found:

$$v_2 = \sqrt{2J(h_1 - h_2) + v_1^2} \quad (3.15a)$$

This equation applies to ideal and non-ideal rockets. For constant  $k$  this expression can be rewritten with the aid of Eqs. 3-6 and 3-7. The subscripts 1 and 2 apply to the nozzle inlet and exit conditions respectively:

$$v_2 = \sqrt{\frac{2k}{k-1} RT_1 \left[ 1 - \left( \frac{p_2}{p_1} \right)^{(k-1)/k} \right] + v_1^2} \quad (3.15b)$$

This equation also holds for any two points within the nozzle. When the chamber section is large compared to the nozzle throat section, the chamber velocity or nozzle approach velocity is comparatively small and the term  $v_1^2$  can be neglected. The chamber temperature  $T_1$  is at the nozzle inlet and, under isentropic conditions, differs little from the stagnation temperature or (for a chemical rocket) from the combustion temperature. This leads to an important simplified expression of the exhaust velocity  $v_2$ , which is often used in the analysis.

$$\begin{aligned} v_2 &= \sqrt{\frac{2k}{k-1} RT_1 \left[ 1 - \left( \frac{p_2}{p_1} \right)^{(k-1)/k} \right]} \\ &= \sqrt{\frac{2k}{k-1} \frac{R' T_0}{\mathfrak{M}} \left[ 1 - \left( \frac{p_2}{p_1} \right)^{(k-1)/k} \right]} \end{aligned} \quad (3-16)$$



It can be seen that the exhaust velocity of a nozzle is a function of the pressure ratio  $p_1/p_2$ , the ratio of specific heats  $k$ , and the absolute temperature at the nozzle inlet  $T_1$ , as well as the gas constant  $R$ . Because the gas constant for any particular gas is inversely proportional to the molecular mass  $\mathfrak{M}$ , the exhaust velocity or the specific impulse are a function of the ratio of the absolute nozzle entrance temperature divided by the molecular mass, as is shown in Fig. 3-2. This ratio plays an important role in optimizing the mixture ratio in chemical rockets.

Equations 2-14 and 2-15 give the relations between the velocity  $v_2$ , the thrust  $F$ , and the specific impulse  $I_s$ ; it is plotted in Fig. 3-2 for two pressure ratios and three values of  $k$ . Equation 3-16 indicates that any increase in the gas temperature (usually caused by an increase in energy release) or any decrease of the molecular mass of the propellant (usually achieved by using light molecular mass gases rich in hydrogen content) will improve the performance of the rocket; that is, they will increase the specific impulse  $I_s$  or the exhaust velocity  $v_2$  or  $c$  and, thus, the performance of the vehicle. The influences of the pressure ratio across the nozzle  $p_1/p_2$  and of the specific heat ratio  $k$  are less pronounced. As can be seen from Fig. 3-2, performance increases

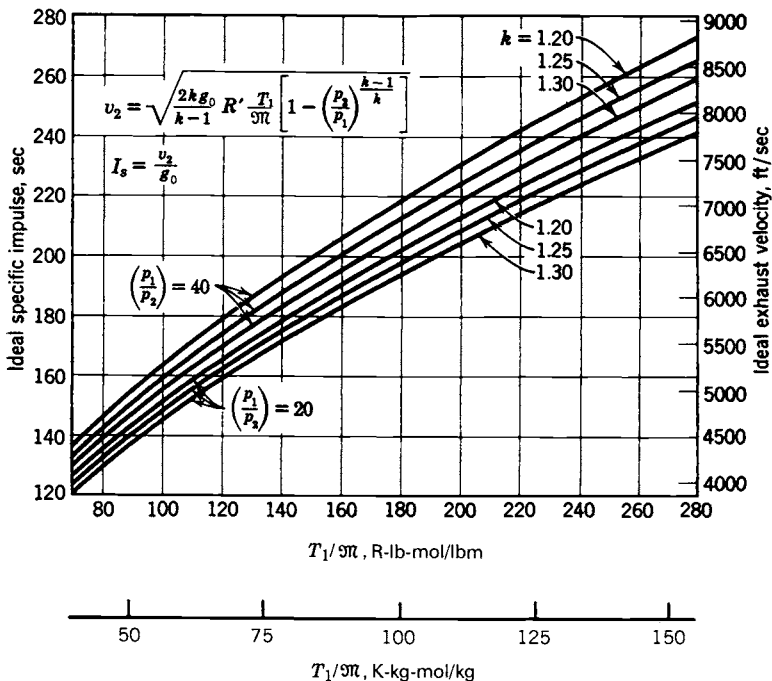


FIGURE 3-2. Specific impulse and exhaust velocity of an ideal rocket at optimum nozzle expansion as functions of the absolute chamber temperature  $T_1$  and the molecular mass  $\mathfrak{M}$  for several values of  $k$  and  $p_1/p_2$ .

with an increase of the pressure ratio; this ratio increases when the value of the chamber pressure  $p_1$  increases or when the exit pressure  $p_2$  decreases, corresponding to high altitude designs. The small influence of  $k$ -values is fortuitous because low molecular masses are found in diatomic or monatomic gases, which have the higher values of  $k$ .

For comparing specific impulse values from one rocket system to another or for evaluating the influence of various design parameters, the value of the pressure ratio must be standardized. A chamber pressure of 1000 psia (6.894 MPa) and an exit pressure of 1 atm (0.1013 MPa) are generally in use today.

For *optimum expansion*  $p_2 = p_3$  and the effective exhaust velocity  $c$  (Eq. 2-16) and the ideal rocket exhaust velocity are related, namely

$$v_2 = (c_2)_{\text{opt}} \quad (3-17)$$

and  $c$  can be substituted for  $v_2$  in Eqs. 3-15 and 3-16. For a fixed nozzle exit area ratio, and constant chamber pressure, this optimum condition occurs only at a particular altitude where the ambient pressure  $p_3$  happens to be equal to the nozzle exhaust pressure  $p_2$ . At all other altitudes  $c \neq v_2$ .

The maximum theoretical value of the nozzle outlet velocity is reached with an infinite expansion (exhausting into a vacuum).

$$(v_2)_{\text{max}} = \sqrt{2kRT_0/(k-1)} \quad (3-18)$$

This maximum theoretical exhaust velocity is finite, even though the pressure ratio is infinite, because it represents the finite thermal energy content of the fluid. Such an expansion does not happen, because, among other things, the temperature of many of the working medium species will fall below their liquefaction or the freezing points; thus they cease to be a gas and no longer contribute to the gas expansion.

**Example 3-2.** A rocket operates at sea level ( $p = 0.1013$  MPa) with a chamber pressure of  $p_1 = 2.068$  MPa or 300 psia, a chamber temperature of  $T_1 = 2222$  K, and a propellant consumption of  $\dot{m} = 1$  kg/sec. (Let  $k = 1.30$ ,  $R = 345.7$  J/kg-K). Show graphically the variation of  $A$ ,  $v$ ,  $V$ , and  $M$ , with respect to pressure along the nozzle. Calculate the ideal thrust and the ideal specific impulse.

**SOLUTION.** Select a series of pressure values and calculate for each pressure the corresponding values of  $v$ ,  $V$ , and  $A$ . A sample calculation is given below. The initial specific volume  $V_1$  is calculated from the equation of state of a perfect gas, Eq. 3-4:

$$V_1 = RT_1/p_1 = 345.7 \times 2222/(2.068 \times 10^6) = 0.3714 \text{ m}^3/\text{kg}$$

In an isentropic flow at a point of intermediate pressure, say at  $p_x = 1.379$  MPa or 200 psi, the specific volume and the temperature are, from Eq. 3-7,

$$V_x = V_1(p_1/p_x)^{1/k} = 0.3714(2.068/1.379)^{1/1.3} = 0.5072 \text{ m}^3/\text{kg}$$

$$T_x = T_1(p_x/p_1)^{(k-1)/k} = 2222(1.379/2.068)^{0.38/1.3} = 2023 \text{ K}$$

The calculation of the velocity follows from Eq. 3-16:

$$v_x = \sqrt{\frac{2kRT_1}{k-1} \left[ 1 - \left( \frac{p_x}{p_1} \right)^{(k-1)/k} \right]}$$

$$= \sqrt{\frac{2 \times 1.30 \times 345.7 \times 2222}{1.30 - 1} \left[ 1 - \left( \frac{1.379}{2.068} \right)^{0.2307} \right]} = 771 \text{ m/sec}$$

The cross-sectional area is found from Eq. 3-3:

$$A_x = \dot{m}_x V_x / v_x = 1 \times 0.5072 / 771 = 658 \text{ cm}^2$$

The Mach number  $M$  is, using Eq. 3-11,

$$M_x = v_x / \sqrt{kRT_x} = 771 / \sqrt{1.30 \times 345.7 \times 1932} = 0.8085$$

Figure 3-3 shows the variations of the velocity, specific volume, area, and Mach number with pressure in this nozzle. At optimum expansion the ideal exhaust velocity  $v_2$  is equal to the effective exhaust velocity  $c$  and, from Eq. 3-16, it is calculated to be 1827 m/sec. Therefore, the thrust  $F$  and the specific impulse can be determined from Eqs. 2-6 and 2-14:

$$F = \dot{m} v_2 = 1 \times 1827 = 1827 \text{ N}$$

$$I_s = c/g_0 = 1827/9.80 = 186 \text{ sec}$$

A number of interesting deductions can be made from this example. Very *high gas velocities* (over 1 km/sec) can be obtained in rocket nozzles. The *temperature drop* of the combustion gases flowing through a rocket nozzle is appreciable. In the example given the temperature changed 1117°C in a relatively short distance. This should not be surprising, for the increase in the kinetic energy of the gases is derived from a decrease of the enthalpy, which in turn is proportional to the decrease in temperature. Because the exhaust gases are still very hot (1105 K) when leaving the nozzle, they contain considerable thermal energy not available for conversion into kinetic energy of the jet.

### Nozzle Flow and Throat Condition

The required nozzle area decreases to a *minimum* (at 1.130 MPa or 164 psi pressure in the previous example) and then increases again. Nozzles of this type (often called De Laval nozzles after their inventor) consist of a convergent section followed by a divergent section. From the continuity equation, the

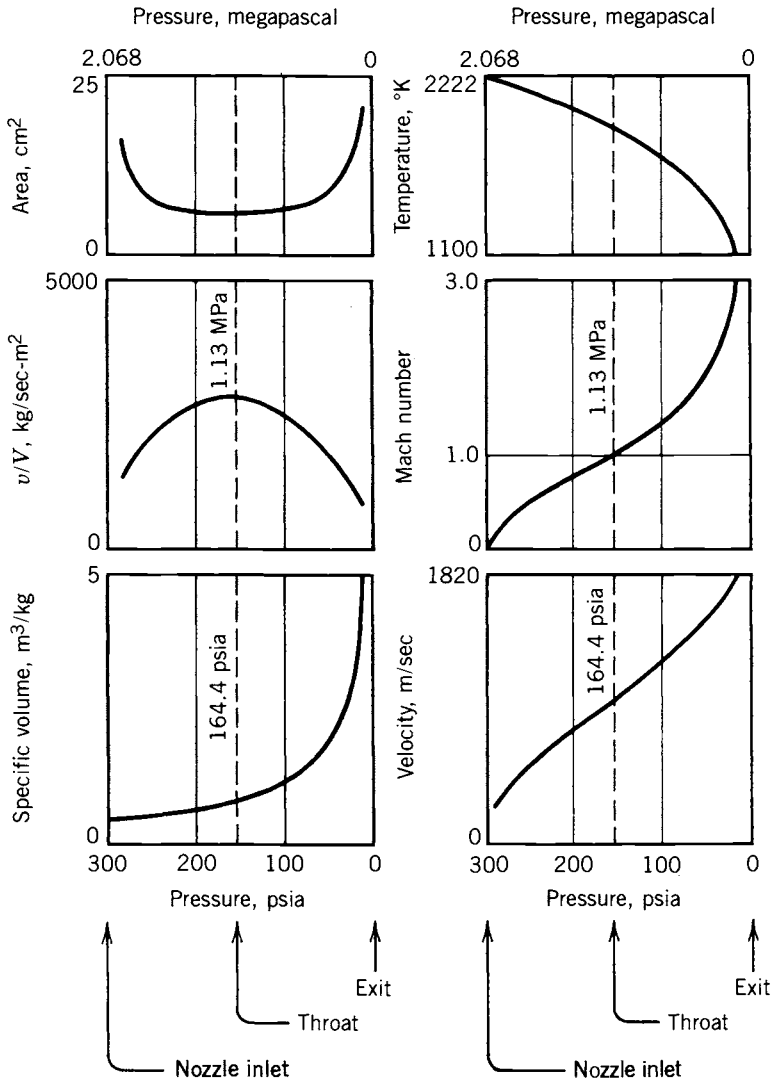


**FIGURE 3-3.** Typical variation of cross-sectional area, temperature, specific volume, and velocity with pressure in a rocket nozzle.

area is inversely proportional to the ratio  $v/V$ . This quantity has also been plotted in Fig. 3-3. There is a maximum in the curve of  $v/V$  because at first the velocity increases at a greater rate than the specific volume; however, in the divergent section, the specific volume increases at a greater rate.

The minimum nozzle area is called the *throat area*. The ratio of the nozzle exit area  $A_2$  to the throat area  $A_1$  is called the nozzle area expansion ratio and is designated by the Greek letter  $\epsilon$ . It is an important nozzle design parameter.

$$\epsilon = A_2/A_t \quad (3-19)$$

The maximum gas flow per unit area occurs at the throat where there is a unique gas pressure ratio which is only a function of the ratio of specific heats  $k$ . This pressure ratio is found by setting  $M = 1$  in Eq. 3-13.

$$p_t/p_1 = [2/(k+1)]^{k/(k-1)} \quad (3-20)$$

The throat pressure  $p_t$  for which the isentropic mass flow rate is a maximum is called the *critical pressure*. Typical values of this critical pressure ratio range between 0.53 and 0.57. The flow through a specified rocket nozzle with a given inlet condition is less than the maximum if the pressure ratio is larger than that given by Eq. 3-20. However, note that this ratio is not that across the entire nozzle and that the maximum flow or choking condition (explained below) is always established internally at the throat and not at the exit plane. The nozzle inlet pressure is very close to the chamber stagnation pressure, except in narrow combustion chambers where there is an appreciable drop in pressure from the injector region to the nozzle entrance region. This is discussed in Section 3.5. At the point of critical pressure, namely the throat, the Mach number is one and the values of the specific volume and temperature can be obtained from Eqs. 3-7 and 3-12.

$$V_t = V_1[(k+1)/2]^{1/(k-1)} \quad (3-21)$$

$$T_t = 2T_1/(k+1) \quad (3-22)$$

In Eq. 3-22 the nozzle inlet temperature  $T_1$  is very close to the combustion temperature and hence close to the nozzle flow stagnation temperature  $T_0$ . At the critical point there is only a mild change of these properties. Take for example a gas with  $k = 1.2$ ; the critical pressure ratio is about 0.56 (which means that  $p_t$  equals almost half of the chamber pressure  $p_1$ ); the temperature drops only slightly ( $T_t = 0.91T_1$ ), and the specific volume expands by over 60% ( $V_t = 1.61V_1$ ). From Eqs. 3-15, 3-20, and 3-22, the critical or throat velocity  $v_t$  is obtained:

$$v_t = \sqrt{\frac{2k}{k+1}} RT_1 = a_t = \sqrt{kRT} \quad (3-23)$$

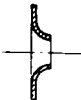
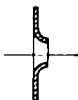
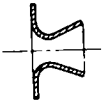
The first version of this equation permits the throat velocity to be calculated directly from the nozzle inlet conditions without any of the throat conditions being known. At the nozzle throat the critical velocity is clearly also the sonic velocity. The divergent portion of the nozzle permits further decreases in pressure and increases in velocity under supersonic conditions. If the nozzle is cut off at the throat section, the exit gas velocity is sonic and the flow rate remains

a maximum. The sonic and supersonic flow condition can be attained only if the critical pressure prevails at the throat, that is, if  $p_2/p_1$  is equal to or less than the quantity defined by Eq. 3-20. There are, therefore, three different types of nozzles: subsonic, sonic, and supersonic, and these are described in Table 3-1.

The supersonic nozzle is the one used for rockets. It achieves a high degree of conversion of enthalpy to kinetic energy. The ratio between the inlet and exit pressures in all rockets is sufficiently large to induce supersonic flow. Only if the absolute chamber pressure drops below approximately 1.78 atm will there be subsonic flow in the divergent portion of the nozzle during sea-level operation. This condition occurs for a very short time during the start and stop transients.

The velocity of sound is equal to the propagation speed of an elastic pressure wave within the medium, sound being an infinitesimal pressure wave. If, therefore, sonic velocity is reached at any point within a steady flow system, it is impossible for a pressure disturbance to travel past the location of sonic or supersonic flow. Thus, any partial obstruction or disturbance of the flow downstream of the nozzle throat with sonic flow has no influence on the throat or upstream of it, provided that the disturbance does not raise the downstream pressure above its critical value. It is not possible to increase the throat velocity or the flow rate in the nozzle by further lowering the exit pressure or even evacuating the exhaust section. This important condition is often described as *choking* the flow. It is always established at the throat and not the nozzle exit plane. *Choked flow* through the critical section of a supersonic nozzle may be derived from Eqs. 3-3, 3-21, and 3-23. It is equal to the mass flow at any section within the nozzle.

TABLE 3-1. Nozzle Types

	Subsonic	Sonic	Supersonic
Throat velocity	$v_1 < a_1$	$v_1 = a_1$	$v_1 = a_1$
Exit velocity	$v_2 < a_2$	$v_2 = v_1$	$v_2 > v_1$
Mach number	$M_2 < 1$	$M_2 = M_1 = 1.0$	$M_2 > 1$
Pressure ratio	$\frac{p_1}{p_2} < \left(\frac{k+1}{2}\right)^{k/(k-1)}$	$\frac{p_1}{p_2} = \frac{p_1}{p_t} = \left(\frac{k+1}{2}\right)^{k/(k-1)}$	$\frac{p_1}{p_2} > \left(\frac{k+1}{2}\right)^{k/(k-1)}$
Shape			

$$\dot{m} = \frac{A_t v_t}{V_t} = A_t p_1 k \frac{\sqrt{[2/(k+1)]^{(k+1)/(k-1)}}}{\sqrt{kRT_1}} \quad (3-24)$$

The mass flow through a rocket nozzle is therefore proportional to the throat area  $A_t$  and the chamber (stagnation) pressure  $p_1$ ; it is also inversely proportional to the square root of  $T/\mathfrak{M}$  and a function of the gas properties. For a supersonic nozzle the *ratio between the throat and any downstream area* at which a pressure  $p_x$  prevails can be expressed as a function of the pressure ratio and the ratio of specific heats, by using Eqs. 3-4, 3-16, 3-21, and 3-23, as follows:

$$\frac{A_t}{A_x} = \frac{V_t v_x}{V_x v_t} = \left(\frac{k+1}{2}\right)^{1/(k-1)} \left(\frac{p_x}{p_1}\right)^{1/k} \sqrt{\frac{k+1}{k-1} \left[1 - \left(\frac{p_x}{p_1}\right)^{(k-1)/k}\right]} \quad (3-25)$$

When  $p_x = p_2$ , then  $A_x/A_t = A_2/A_t = \epsilon$  in Eq. 3-25. For low-altitude operation (sea level to about 10,000 m) the nozzle area ratios are typically between 3 and 25, depending on chamber pressure, propellant combinations, and vehicle envelope constraints. For high altitude (100 km or higher) area ratios are typically between 40 and 200, but there have been some as high as 400. Similarly, an expression for the ratio of the velocity at any point downstream of the throat with the pressure  $p_x$ , and the throat velocity may be written from Eqs. 3-15 and 3-23:

$$\frac{v_x}{v_t} = \sqrt{\frac{k+1}{k-1} \left[1 - \left(\frac{p_x}{p_1}\right)^{(k-1)/k}\right]} \quad (3-26)$$

These equations permit the direct determination of the velocity ratio or the area ratio for any given pressure ratio, and vice versa, in ideal rocket nozzles. They are plotted in Figs. 3-4 and 3-5, and these plots allow the determination of the pressure ratios given the area or velocity ratios. When  $p_x = p_2$ , Eq. 3-26 describes the velocity ratio between the nozzle exit area and the throat section. When the exit pressure coincides with the atmospheric pressure ( $p_2 = p_3$ , see Fig. 2-1), these equations apply for optimum nozzle expansion. For rockets that operate at high altitudes, not too much additional exhaust velocity can be gained by increasing the area ratio above 1000. In addition, design difficulties and a heavy inert nozzle mass make applications above area ratios of about 350 marginal.

Appendix 2 is a table of several properties of the Earth's atmosphere with agreed-upon standard values. It gives ambient pressure for different altitudes. These properties can vary somewhat from day to day (primarily because of solar activity) and between hemispheres. For example, the density of the atmosphere at altitudes between 200 and 3000 km can change by more than an order of magnitude, affecting satellite drag.

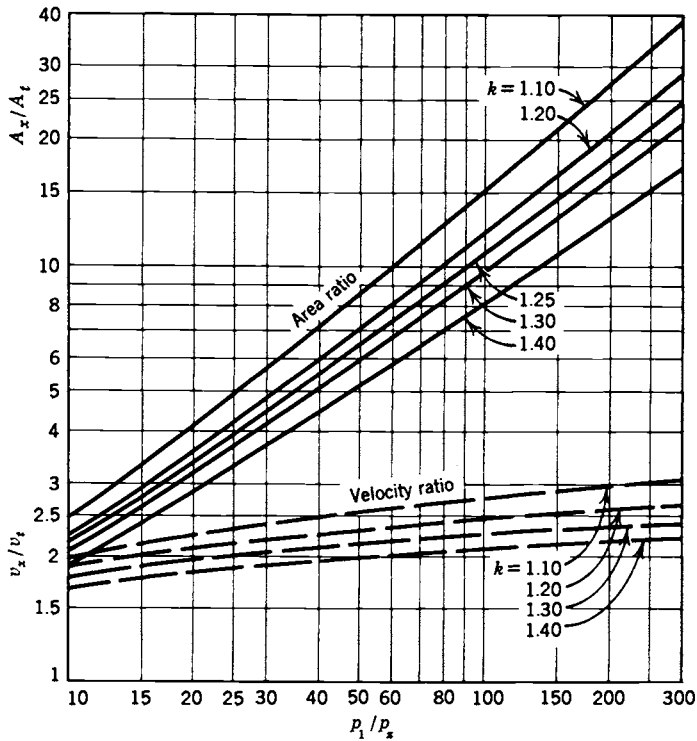


**FIGURE 3-4.** Area and velocity ratios as function of pressure ratio for the diverging section of a supersonic nozzle.

**Example 3-3.** Design a nozzle for an ideal rocket that has to operate at 25 km altitude and give 5000 N thrust at a chamber pressure of 2.068 MPa and a chamber temperature of 2800 K. Assuming that  $k = 1.30$  and  $R = 355.4$  J/kg-K, determine the throat area, exit area, throat velocity, and exit temperature.

**SOLUTION.** At 25 km the atmospheric pressure equals 0.002549 MPa (in Appendix 2 the ratio is 0.025158 which must be multiplied by the pressure at sea level or 0.1013 MPa). The pressure ratio is

$$p_2/p_1 = p_3/p_1 = 0.002549/2.068 = 0.001232 = 1/811.3$$

The critical pressure, from Eq. 3-20, is

$$p_t = 0.546 \times 2.068 = 1.129 \text{ MPa}$$

The throat velocity, from Eq. 3-23, is

$$v_t = \sqrt{\frac{2k}{k+1} RT_1} = \sqrt{\frac{2 \times 1.30}{1.3 + 1} 355.4 \times 2800} = 1060 \text{ m/sec}$$



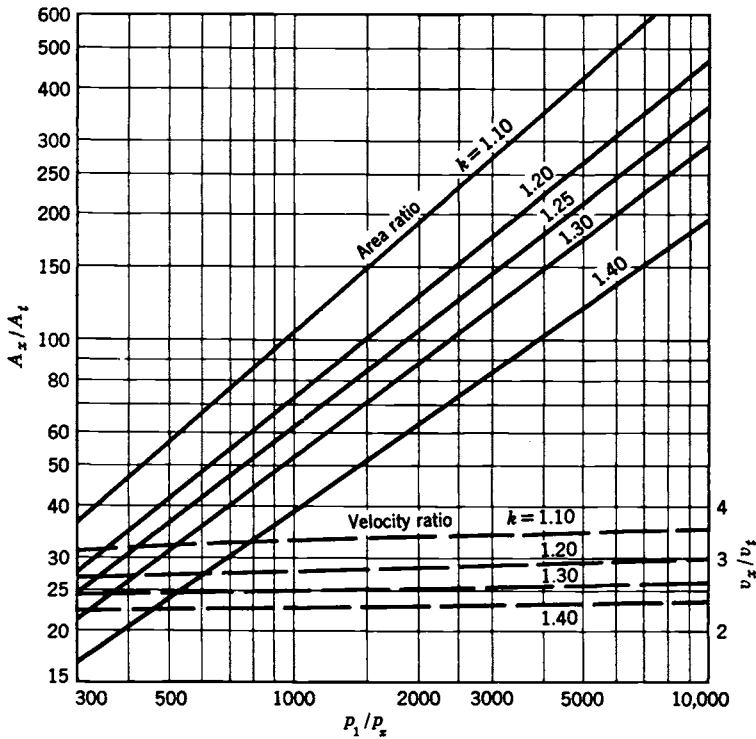


**FIGURE 3-5.** Continuation of prior figure of area ratios and velocity ratios, but for higher pressure ratios in a supersonic nozzle.

The ideal exit velocity is found from Eq. 3-16 or Fig. 3-5, using a pressure ratio of 811.3:

$$\begin{aligned}
 v_2 &= \sqrt{\frac{2k}{k-1} RT_1 \left[ 1 - \left( \frac{p_2}{p_1} \right)^{(k-1)/k} \right]} \\
 &= \sqrt{\frac{2 \times 1.30}{1.30 - 1} 355.4 \times 2800 \times 0.7869} = 2605 \text{ m/sec}
 \end{aligned}$$

An approximate value of this velocity can also be obtained from the throat velocity and Fig. 3-4. The ideal propellant consumption for optimum expansion conditions is

$$\dot{m} = F/v_2 = 5000/2605 = 1.919 \text{ kg/sec}$$

The specific volume at the entrance to the nozzle equals

$$V_1 = RT_1/p_1 = 355.4 \times 2800 / (2.068 \times 10^6) = 0.481 \text{ m}^3/\text{kg}$$

At the throat and exit sections the specific volumes are obtained from Eqs. 3-21 and 3-7:

$$V_t = V_1 \left( \frac{k+1}{2} \right)^{1/(k-1)} = 0.481 \left( \frac{2.3}{2} \right)^{1/0.3} = 0.766 \text{ m}^3/\text{kg}$$

$$V_2 = V_1 \left( \frac{p_1}{p_2} \right)^{1/k} = 0.481 (2.068/0.002549)^{0.7692} = 83.15 \text{ m}^3/\text{kg}$$

The areas at the throat and exit sections and the nozzle area ratio  $A_2/A_t$  are

$$A_t = \dot{m} V_t / v_t = 1.919 \times 0.766 / 1060 = 13.87 \text{ cm}^2$$

$$A_2 = \dot{m} V_2 / v_2 = 1.919 \times 83.15 / 2605 = 612.5 \text{ cm}^2$$

$$\epsilon = A_2 / A_t = 612.5 / 13.87 = 44.16$$

An approximate value of this area ratio can also be obtained directly from Fig. 3-5 for  $k = 1.30$  and  $p_1/p_2 = 811.2$ . The exit temperature is given by

$$T_2 = T_1 (p_2/p_1)^{(k-1)/k} = 2800 (0.002549/2.068)^{0.2307} = 597 \text{ K}$$

### Thrust and Thrust Coefficient

The efflux of the propellant gases or the momentum flux-out causes the thrust or reaction force on the rocket structure. Because the flow is supersonic, the pressure at the exit plane of the nozzle may be different from the ambient pressure and the pressure thrust component adds to the momentum thrust as given by Eq. 2-14:

$$F = \dot{m} v_2 + (p_2 - p_3) A_2 \quad (2-14)$$

The maximum thrust for any given nozzle operation is found in a vacuum where  $p_3 = 0$ . Between sea level and the vacuum of space, Eq. 2-14 gives the variation of thrust with altitude, using the properties of the atmosphere such as those listed in Appendix 2. Figure 2-2 shows a typical variation of thrust with altitude. To modify values calculated for optimum operating conditions ( $p_2 = p_3$ ) for given values of  $p_1$ ,  $k$ , and  $A_2/A_t$ , the following expressions may be used. For the thrust,

$$F = F_{\text{opt}} + p_1 A_t \left( \frac{p_2}{p_1} - \frac{p_3}{p_1} \right) \frac{A_2}{A_t} \quad (3-27)$$

For the specific impulse, using Eqs. 2-5, 2-18, and 2-14,

$$I_s = (I_s)_{\text{opt}} + \frac{c^* \epsilon}{g_0} \left( \frac{p_2}{p_1} - \frac{p_3}{p_1} \right) \quad (3-28)$$

If, for example, the specific impulse for a new exit pressure  $p_2$  corresponding to a new area ratio  $A_2/A_t$  is to be calculated, the above relations may be used.

Equation 2-14 can be expanded by modifying it and substituting  $v_2$ ,  $v_t$  and  $V_t$  from Eqs. 3-16, 3-21, and 3-23.

$$\begin{aligned} F &= \frac{A_t v_t v_2}{V_t} + (p_2 - p_3)A_2 \\ &= A_t p_1 \sqrt{\frac{2k^2}{k-1} \left( \frac{2}{k+1} \right)^{(k+1)/(k-1)} \left[ 1 - \left( \frac{p_2}{p_1} \right)^{(k-1)/k} \right]} + (p_2 - p_3)A_2 \end{aligned} \quad (3-29)$$

The first version of this equation is general and applies to all rockets, the second form applies to an ideal rocket with  $k$  being constant throughout the expansion process. This equation shows that the thrust is proportional to the throat area  $A_t$  and the chamber pressure (or the nozzle inlet pressure)  $p_1$  and is a function of the pressure ratio across the nozzle  $p_1/p_2$ , the specific heat ratio  $k$ , and of the pressure thrust. It is called the ideal thrust equation. The thrust coefficient  $C_F$  is defined as the thrust divided by the chamber pressure  $p_1$  and the throat area  $A_t$ . Equations 2-14, 3-21, and 3-16 then give

$$\begin{aligned} C_F &= \frac{v_2^2 A_2}{p_1 A_t V_2} + \frac{p_2 A_2}{p_1 A_t} - \frac{p_3 A_2}{p_1 A_t} \\ &= \sqrt{\frac{2k^2}{k-1} \left( \frac{2}{k+1} \right)^{(k+1)/(k-1)} \left[ 1 - \left( \frac{p_2}{p_1} \right)^{(k-1)/k} \right]} + \frac{p_2 - p_3}{p_1} \frac{A_2}{A_t} \end{aligned} \quad (3-30)$$

The thrust coefficient  $C_F$  is a function of gas property  $k$ , the nozzle area ratio  $\epsilon$ , and the pressure ratio across the nozzle  $p_1/p_2$ , but independent of chamber temperature. For any fixed pressure ratio  $p_1/p_3$ , the thrust coefficient  $C_F$  and the thrust  $F$  have a peak when  $p_2 = p_3$ . This peak value is known as the *optimum thrust coefficient* and is an important criterion in nozzle design considerations. The use of the thrust coefficient permits a simplification to Eq. 3-29:

$$F = C_F A_t p_1 \quad (3-31)$$

Equation 3-31 can be solved for  $C_F$  and provides the relation for determining the thrust coefficient experimentally from measured values of chamber pressure, throat diameter, and thrust. Even though the thrust coefficient is a function of chamber pressure, it is not simply proportional to  $p_1$ , as can be seen from Eq. 3-30. However, it is directly proportional to throat area. The thrust coefficient can be thought of as representing the amplification of thrust due to the gas expanding in the supersonic nozzle as compared to the thrust that would be exerted if the chamber pressure acted over the throat area only.

The thrust coefficient has values ranging from about 0.8 to 1.9. It is a convenient parameter for seeing the effects of chamber pressure or altitude variations in a given nozzle configuration, or to correct sea-level results for flight altitude conditions.

Figure 3-6 shows the variation of the *optimum expansion* ( $p_2 = p_3$ ) thrust coefficient for different pressure ratios  $p_1/p_2$ , values of  $k$ , and area ratio  $\epsilon$ . The complete thrust coefficient is plotted in Figs 3-7 and 3-8 as a function of pressure ratio  $p_1/p_3$  and area ratio for  $k = 1.20$  and  $1.30$ . These two sets of curves are useful in solving various nozzle problems for they permit the evaluation of under- and over-expanded nozzle operation, as explained below. The values given in these figures are ideal and do not consider such losses as divergence, friction or internal expansion waves.

When  $p_1/p_3$  becomes very large (e.g., expansion into near-vacuum), then the thrust coefficient approaches an asymptotic maximum as shown in Figs. 3-7 and 3-8. These figures also give values of  $C_F$  for any mismatched nozzle ( $p_2 \neq p_3$ ), provided the nozzle is flowing full at all times, that is, the working fluid does not separate or break away from the walls. Flow separation is discussed later in this section.

### Characteristic Velocity and Specific Impulse

The *characteristic velocity*  $c^*$  was defined by Eq. 2-18. From Eqs. 3-24 and 3-31 it can be shown that

$$c^* = \frac{p_1 A_t}{\dot{m}} = \frac{I_{sg0}}{C_F} = \frac{c}{C_F} = \frac{\sqrt{kRT_1}}{k\sqrt{[2/(k+1)]^{(k+1)/(k-1)}}} \quad (3-32)$$

It is basically a function of the propellant characteristics and combustion chamber design; it is independent of nozzle characteristics. Thus, it can be used as a figure of merit in comparing propellant combinations and combustion chamber designs. The first version of this equation is general and allows the determination of  $c^*$  from experimental data of  $\dot{m}$ ,  $p_1$ , and  $A_t$ . The last version gives the maximum value of  $c^*$  as a function of gas properties, namely  $k$ , the chamber temperature, and the molecular mass  $\mathfrak{M}$ , as determined from the theory in Chapter 5. Some values of  $c^*$  are shown in Tables 5-4 and 5-5. The term *c\*-efficiency* is sometimes used to express the degree of completion of the energy release and the creation of high temperature, high pressure gas in the chamber. It is the ratio of the actual value of  $c^*$ , as determined from measurements, and the theoretical value (last part of Eq. 3-32), and typically has a value between 92 and 99.5 percent.

Using Eqs. 3-31 and 3-32, the thrust itself may now be expressed as the mass flow rate times a function of the combustion chamber ( $c^*$ ) times a function of the nozzle expansion ( $C_F$ ),

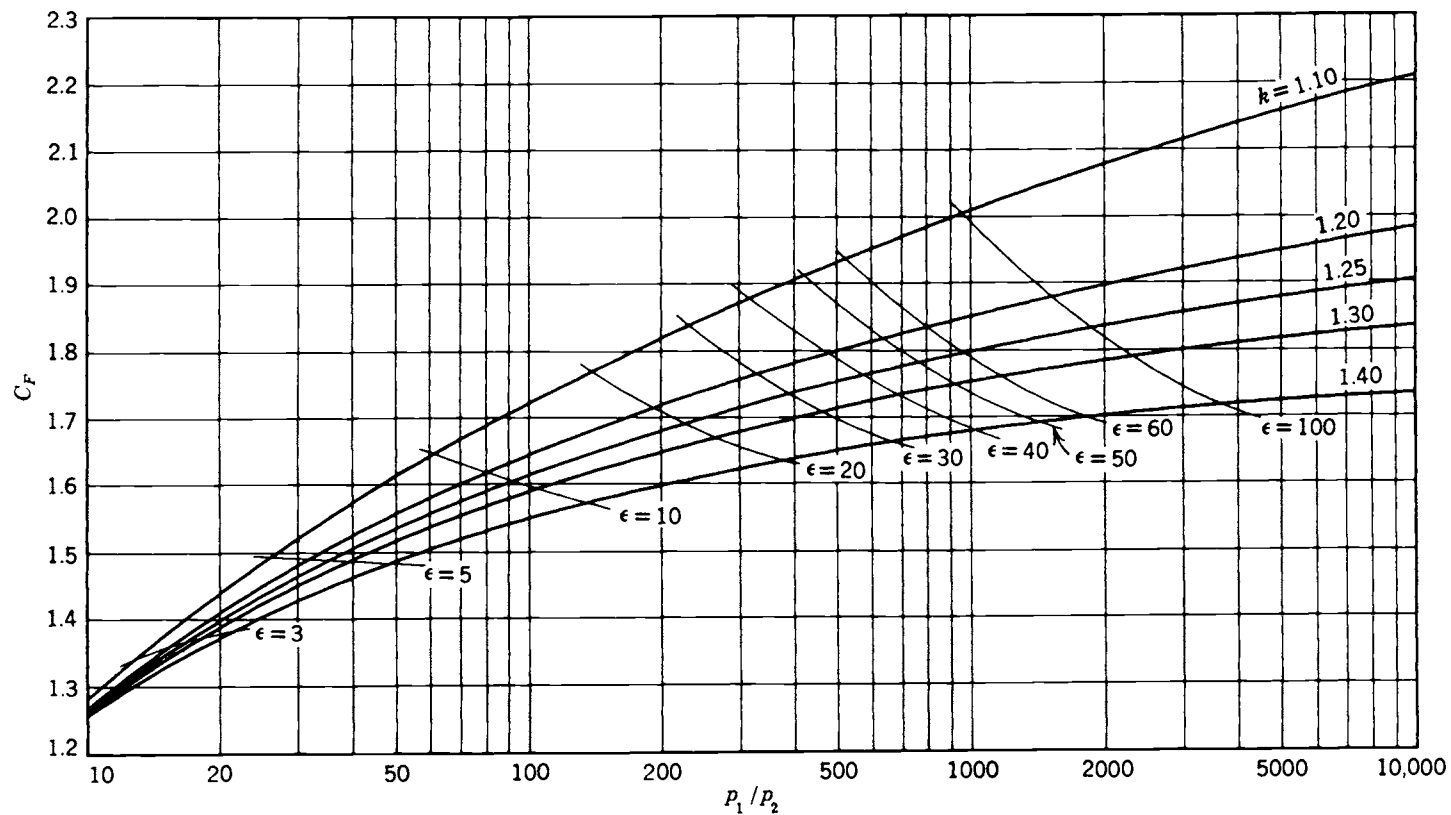


FIGURE 3-6. Thrust coefficient  $C_F$  as a function of pressure ratio, nozzle area ratio, and specific heat ratio for optimum expansion conditions ( $p_2 = p_3$ ).

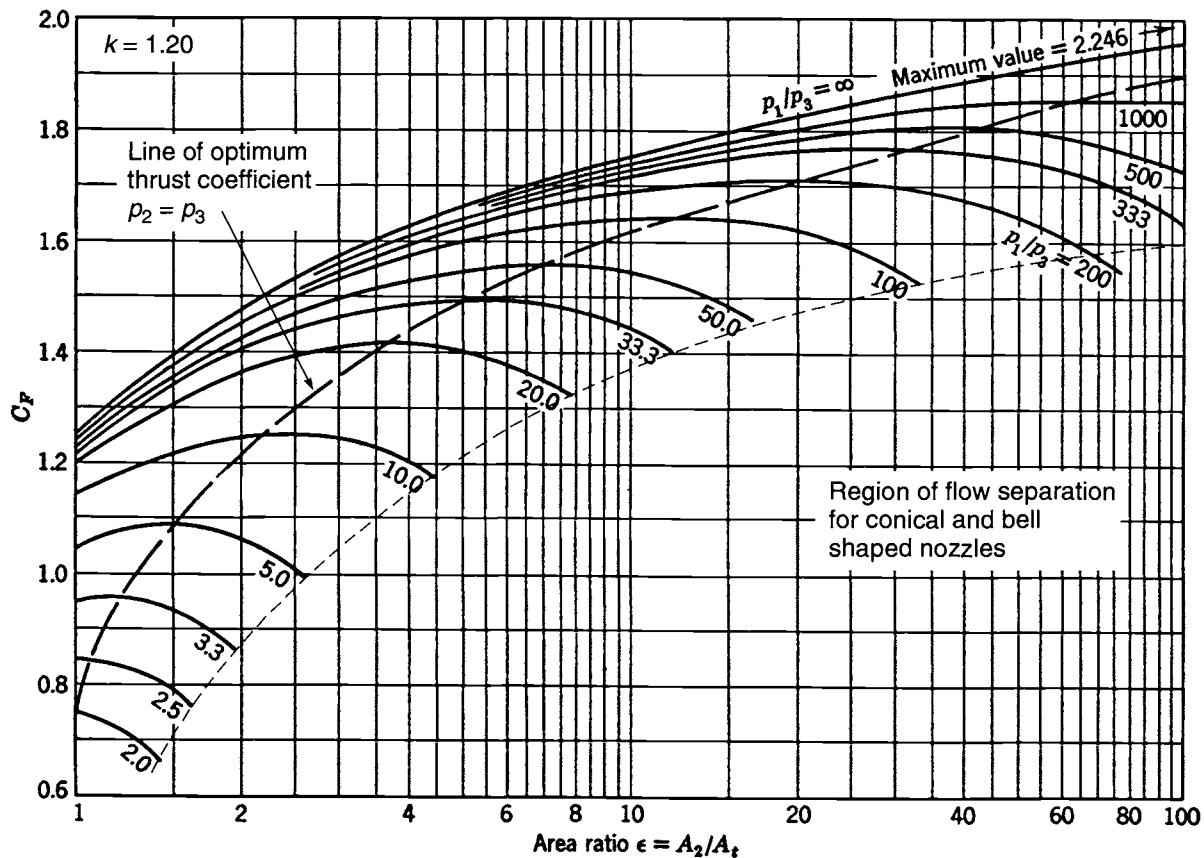


FIGURE 3-7. Thrust coefficient  $C_F$  versus nozzle area ratio for  $k = 1.20$ .

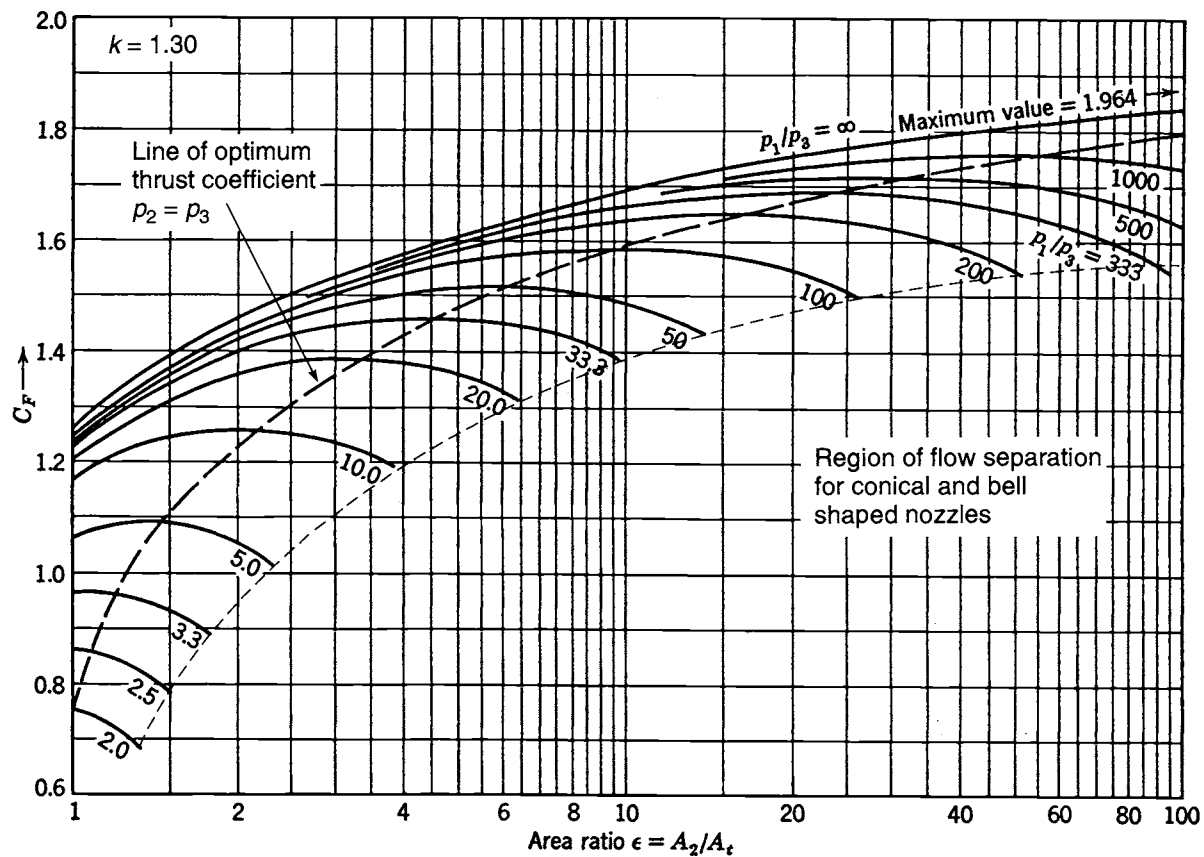


FIGURE 3-8. Thrust coefficient  $C_F$  versus nozzle area ratio for  $k = 1.30$ .

$$F = C_F \dot{m} c^* \quad (3-33)$$

Some authors use a term called the *discharge coefficient*  $C_D$  which is merely the reciprocal of  $c^*$ . Both  $C_D$  and the characteristic exhaust velocity  $c^*$  are used primarily with chemical rocket propulsion systems.

The influence of *variations in the specific heat ratio*  $k$  on various parameters (such as  $c$ ,  $c^* A_2/A_t$ ,  $v_2/v_t$ , or  $I_s$ ) is not as large as the changes in chamber temperature, pressure ratio, or molecular mass. Nevertheless, it is a noticeable factor, as can be seen by examining Figs. 3-2 and 3-4 to 3-8. The value of  $k$  is 1.67 for monatomic gases such as helium and argon, 1.4 for cold diatomic gases such as hydrogen, oxygen, and nitrogen, and for triatomic and beyond it varies between 1.1 and 1.3 (methane is 1.11 and ammonia and carbon dioxide 1.33). In general, the more complex the molecule the lower the value of  $k$ ; this is also true for molecules at high temperatures when their vibrational modes have been activated. The average values of  $k$  and  $\mathfrak{M}$  for typical rocket exhaust gases with several constituents depend strongly on the composition of the products of combustion (chemical constituents and concentrations), as explained in Chapter 5. Values of  $k$  and  $\mathfrak{M}$  are given in Tables 5-4, 5-5, and 5-6.

**Example 3-4.** What is percentage variation in thrust between sea level and 25 km for a rocket having a chamber pressure of 20 atm and an expansion area ratio of 6? (Use  $k = 1.30$ .)

**SOLUTION.** At sea level:  $p_1/p_3 = 20/1.0 = 20$ ; at 25 km:  $p_1/p_3 = 20/0.0251 = 754$  (see Appendix 2).

Use Eq. 3-30 or Fig. 3-8 to determine the thrust coefficient (hint: use a vertical line on Fig. 3-8 corresponding to  $A_2/A_t = 6.0$ ). At sea level:  $C_F = 1.33$ . At 25 km:  $C_F = 1.64$ .

The thrust increase =  $(1.64 - 1.33)/1.33 = 23\%$ .

## Under- and Over-Expanded Nozzles

An *under-expanded nozzle* discharges the fluid at an exit pressure greater than the external pressure because the exit area is too small for an optimum area ratio. The expansion of the fluid is therefore incomplete within the nozzle, and must take place outside. The nozzle exit pressure is higher than the local atmospheric pressure.

In an *over-expanded nozzle* the fluid attains a lower exit pressure than the atmosphere as it has an exit area too large for optimum. The phenomenon of over-expansion for a supersonic nozzle is shown in Fig. 3-9, with typical pressure measurements of superheated steam along the nozzle axis and different back pressures or pressure ratios. Curve  $AB$  shows the variation of pressure with the optimum back pressure corresponding to the area ratio. Curves  $AC$  and  $AD$  show the variation of pressure along the axis for increasingly higher external pressures. The expansion within the nozzle proceeds normally for the



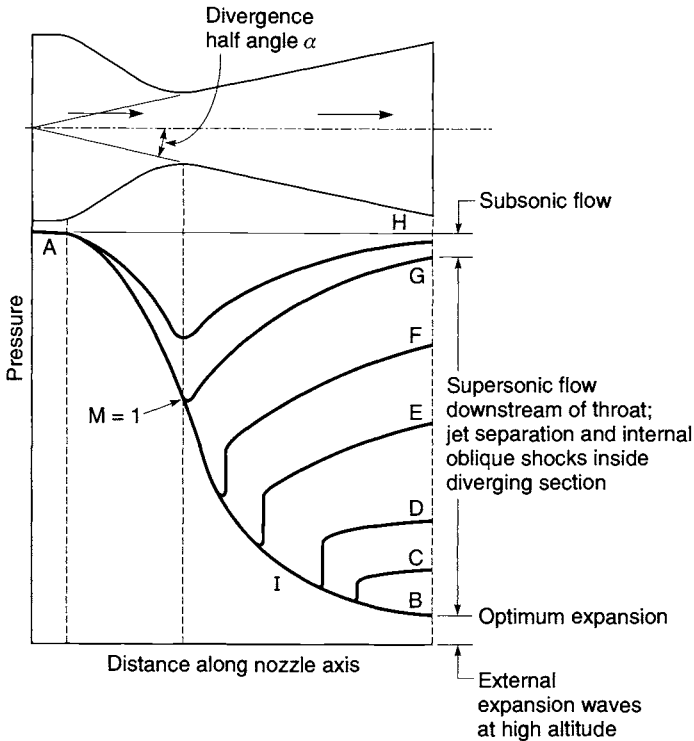


**FIGURE 3-9.** Distribution of pressures in a converging-diverging nozzle for different flow conditions. Inlet pressure is the same, but exit pressure changes. Based on experimental data from A. Stodala.

initial portion of the nozzle. At point *I* on curve *AD*, for example, the pressure is lower than the exit pressure and a sudden rise in pressure takes place which is accompanied by the *separation* of the flow from the walls (separation is described later).

The non-ideal behavior of nozzles is strongly influenced by the presence of compression waves or shock waves inside the diverging nozzle section, which are strong compression discontinuities and exist only in supersonic flow. The sudden pressure rise in the curve *ID* is such a compression wave. Expansion waves, also strictly supersonic phenomena, match the flow from a nozzle exit to lower ambient pressures. Compression and expansion waves are described in Chapter 18.

The different possible flow conditions in a supersonic nozzle are as follows:

1. When the external pressure  $p_3$  is below the nozzle exit pressure  $p_2$ , the nozzle will flow full but will have external expansion waves at its exit (i.e., under-expansion). The expansion of the gas inside the nozzle is incomplete and the value of  $C_F$  and  $I_s$  will be less than at optimum expansion.

2. For external pressures  $p_3$  slightly higher than the nozzle exit pressure  $p_2$ , the nozzle will continue to flow full. This occurs until  $p_2$  reaches a value between about 25 and 40% of  $p_3$ . The expansion is somewhat inefficient and  $C_F$  and  $I_s$  will have lower values than an optimum nozzle would have. Shock waves will exist outside the nozzle exit section.
3. For higher external pressures, separation of the flow will take place inside the divergent portion of the nozzle. The diameter of the supersonic jet will be smaller than the nozzle exit diameter. With steady flow, separation is typically axially symmetric. Figs. 3-10 and 3-11 show diagrams of separated flows. The axial location of the separation plane depends on the local pressure and the wall contour. The point of separation travels downstream with decreasing external pressure. At the nozzle exit the flow in the center portion remains supersonic, but is surrounded by an annular shaped section of subsonic flow. There is a discontinuity at the separation location and the thrust is reduced, compared to a nozzle that would have been cut off at the separation plane. Shock waves exist outside the nozzle in the external plume.
4. For nozzles in which the exit pressure is just below the value of the inlet pressure, the pressure ratio is below the critical pressure ratio (as defined by Eq. 3-20) and subsonic flow prevails throughout the entire nozzle. This condition occurs normally in rocket nozzles for a short time during the start and stop transients.

The method for estimating pressure at the location of the separation plane inside the diverging section of a supersonic nozzle has usually been empirical. Reference 3-4 shows separation regions based on collected data for several dozen actual conical and bell-shaped nozzles during separation. Reference 3-5 describes a variety of nozzles, their behavior, and methods used to estimate the location and the pressure at separation. Actual values of pressure for the over-expanded and under-expanded regimes described above are functions of the specific heat ratio and the area ratio (see Ref. 3-1).

The axial thrust direction is not usually altered by separation, because a steady flow usually separates uniformly over a cross-section in a divergent nozzle cone of conventional rocket design. During transients, such as start and stop, the separation may not be axially symmetric and may cause momentary but large side forces on the nozzle. During a normal sea-level transient of a large rocket nozzle (before the chamber pressure reaches its full value) some momentary flow oscillations and non-symmetric separation of the jet can occur during over-expanded flow operation. Reference 3-4 shows that the magnitude and direction of transient side forces can change rapidly and erratically. The resulting side forces can be large and have caused failures of nozzle exit cone structures and thrust vector control gimbal actuators. References 3-5 and 3-6 discuss techniques for estimating these side forces.

When the flow separates, as it does in a highly over-expanded nozzle, the thrust coefficient  $C_F$  can be estimated if the point of separation in the nozzle is

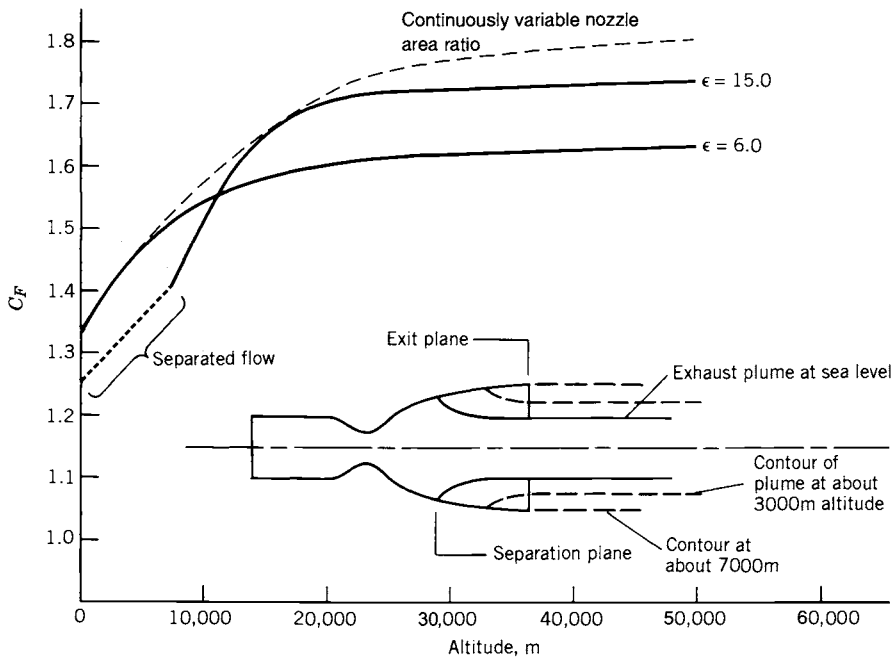
known. Thus,  $C_F$  can be determined for an equivalent smaller nozzle with an exit area equal to that at the point of separation. The effect of separation is to increase the thrust and the thrust coefficient over the value that they would have if separation had not occurred. Thus, with separated gas flow, a nozzle designed for high altitude (large value of  $\epsilon$ ) would have a larger thrust at sea level than expected, but not as good as an optimum nozzle; in this case separation may actually be desirable. With separated flow a large and usually heavy portion of the nozzle is not utilized and the nozzle is bulkier and longer than necessary. The added engine weight and size decrease flight performance. Designers therefore select an area ratio that will not cause separation.

Because of uneven flow separation and potentially destructive side loads, sea-level static tests of an upper stage or a space propulsion system with a high area ratio over-expanded nozzle are usually avoided; instead, a sea-level test nozzle with a much smaller area ratio is substituted. However, actual and simulated altitude testing (in an altitude test facility similar to the one described in Chapter 20) would be done with a nozzle having the correct large area ratio. The ideal solution that avoids separation at low altitudes and has high values of  $C_F$  at high altitudes is a nozzle that changes area ratio in flight. This is discussed at the end of this section.

For most applications, the rocket system has to operate over a range of altitudes; for a fixed chamber pressure this implies a range of nozzle pressure ratios. The condition of optimum expansion ( $p_2 = p_3$ ) occurs only at one altitude, and a nozzle with a fixed area ratio is therefore operating much of the time at either over-expanded or under-expanded conditions. The best nozzle for such an application is not necessarily one that gives optimum nozzle gas expansion, but one that gives the largest vehicle flight performance (say, total impulse, or specific impulse, or range, or payload); it can often be related to a time average over the powered flight trajectory.

**Example 3-5.** Use the data from Example 3-4 ( $p_1 = 20$  atm,  $\epsilon = 6.0$ ,  $k = 1.30$ ) but instead use an area ratio of 15. Compare the altitude performance of the two nozzles with different  $\epsilon$  by plotting their  $C_F$  against altitude. Assume no shocks inside the nozzle.

**SOLUTION.** For the  $\epsilon = 15$  case, the optimum pressure ratio  $p_1/p_3 = p_1/p_2$ , and from Fig. 3-6 or 3-8 this value is about 180;  $p_3 = 20/180 = 0.111$  atm, which occurs at about 1400 m altitude. Below this altitude the nozzle is over-expanded. At sea level,  $p_1/p_3 = 20$  and  $p_3 = 1$  atm. As shown in Fig. 3-10, separation would occur. From other similar nozzles it is estimated that separation will occur approximately at a cross-section where the total pressure is about 40% of  $p_3$ , or 0.4 atm. The nozzle would not flow full below an area ratio of about 6 or 7 and the gas jet would only be in the center of the exit area. Weak shock waves and jet contraction would then raise the exhaust jet's pressure to match the one atmosphere external pressure. If the jet had not separated, it would have reached an exit pressure of 0.11 atm, but this is an unstable condition that could not be maintained at sea level. As the vehicle gains altitude, the separation plane would





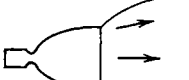
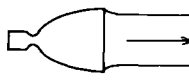


**FIGURE 3-10.** Thrust coefficient  $C_F$  for two nozzles with different area ratios. One has jet separation below about 7000 m altitude. The fully expanded exhaust plume is not shown in the sketch.

gradually move downstream until, at an altitude of about 7000 m, the exhaust gases would occupy the full nozzle area.

The values of  $C_F$  can be obtained by following a vertical line for  $\epsilon = 15$  and  $\epsilon = 6$  in Fig. 3-8 for different pressure ratios, which correspond to different altitudes. Alternatively, Eq. 3-30 can be used for better accuracy. Results are similar to those plotted in Fig. 3-10. The lower area ratio of 6 gives a higher  $C_F$  at low altitudes, but is inferior at the higher altitudes. The larger nozzle gives a higher  $C_F$  at higher altitudes.

Figure 3-11 shows a comparison of altitude and sea-level behavior of three nozzles and their plumes at different area ratios for a typical three-stage satellite launch vehicle. When fired at sea-level conditions, the nozzle of the third stage with the highest area ratio will experience flow separation and suffer a major performance loss; the second stage will flow full but the external plume will contrast; since  $p_2 < p_3$  there is a loss in  $I_s$  and  $F$ . There is no effect on the first stage nozzle.

**Example 3-6.** A rocket engine test gives the following data: thrust  $F = 53,000$  lbf, propellant flow  $\dot{m} = 208$  lbm/sec, nozzle exit area ratio  $A_2/A_t = 10.0$ , atmospheric

Stage	$A_2/A_t$	During flight		During sealevel static tests	
		$h(\text{km})$	$I_s(\text{sec})$	$h(\text{km})$	$I_s(\text{sec})$
Booster or first stage	6	 Nozzle flows full, slight underexpansion	0 267	 Nozzle flows full	0 267
Second stage	10	 Underexpansion	24 312	 Overexpansion, slight contraction	0 254
Third stage	40	 Underexpansion	100 334	 Flow separation caused by overexpansion	0 245

**FIGURE 3-11.** Simplified sketches of exhaust gas behavior of three typical rocket nozzles for a three-stage launch vehicle. The first vehicle stage has the biggest chamber and the highest thrust but the lowest nozzle area ratio, and the top or third stage usually has the lower thrust but the highest nozzle area ratio.

pressure at test station (the nozzle flows full)  $p_3 = 13.8$  psia, and chamber pressure  $p_1 = 620$  psia. The test engineer also knows that the theoretical specific impulse is 289 sec at the standard reference conditions of  $p_1 = 1000$  psia and  $p_3 = 14.7$  psia, and that  $k = 1.20$ . Correct the value of the thrust to sea-level expansion and the specific impulse corresponding. Assume the combustion temperature and  $k$  do not vary significantly with chamber pressure; this is realistic for certain propellants.

**SOLUTION.** The actual pressure ratio was  $p_1/p_3 = 620/13.8 = 44.9$ ; the ideal pressure ratio at standard conditions would have been equal to  $1000/14.7 = 68.0$  and the actual pressure ratio for expansion to sea level would have been  $620/14.7 = 42.1$ . The thrust coefficient for the test conditions is obtained from Fig. 3-7 or from Eq. 3-30 as  $C_F = 1.52$  (for  $p_1/p_3 = 44.9$ ,  $\epsilon = 10$  and  $k = 1.20$ ). The thrust coefficient for the corrected sea-level conditions is similarly found to be 1.60. The thrust at sea level would have been  $F = 53,000 (1.60/1.52) = 55,790$  lbf. The specific impulse would have been

$$I_s = F/\dot{w} = 53,000/208(1.60/1.52) = 268 \text{ sec}$$

The specific impulse can be corrected in proportion to the thrust coefficient because  $k$ ,  $T$ , and therefore  $c^*$  do not vary with  $p_1$ ;  $I_s$  is proportional to  $c$  if  $\dot{m}$  remains constant. The theoretical specific impulse is given for optimum expansion, i.e., for a nozzle area ratio other than 10.0. From Fig. 3-6 or 3-7 and for  $p_1/p_2 = 68.0$  the thrust coefficient is 1.60 and its optimum area ratio approximately 9.0. The corrected specific impulse is accordingly  $255 (1.60/1.51) = 270$  sec. In comparison with the theoretical specific impulse of 289 sec, this rocket has achieved 270/289 or 93.5% of its maximum performance.

Figs. 3-10 and 3-11 suggest that an ideal design for an ascending (e.g., launch) rocket vehicle would have a "rubber-like" diverging section that could be lengthened so that the nozzle exit area could be made larger as the ambient pressure is reduced. The design would then allow the rocket vehicle to attain its maximum performance at all altitudes as it ascends. As yet we have not achieved a simple mechanical hardware design with this full altitude compensation similar to "stretching rubber." However, there are a number of practical nozzle configurations that can be used to alter the flow shape with altitude and obtain maximum performance. They are discussed in the next section.

### Influence of Chamber Geometry

When the chamber has a cross section that is larger than about four times the throat area ( $A_1/A_t > 4$ ), the chamber velocity  $v_1$ , can be neglected, as was mentioned in explaining Eqs. 3-15 and 3-16. However, vehicle space or weight constraints often require smaller thrust chamber areas for liquid propellant engines and grain design considerations lead to small void volumes or small perforations or port areas for solid propellant motors. Then  $v_1$  can no longer be neglected as a contribution to the performance. The gases in the chamber expand as heat is being added. The energy necessary to accelerate these expanding gases within the chamber will also cause a pressure drop and an additional energy loss. This acceleration process in the chamber is adiabatic (no heat transfer) but not isentropic. This loss is a maximum when the chamber diameter is equal to the nozzle diameter, which means that there is no converging nozzle section. This has been called a *throatless rocket motor* and has been used in a few tactical missile booster applications, where there was a premium on minimum inert mass and length. The flight performance improvement due to inert mass savings supposedly outweighs the nozzle performance loss of a throatless motor. Table 3-2 lists some of the performance penalties for three chamber area ratios.

Because of this pressure drop within narrow chambers, the chamber pressure is lower at the nozzle entrance than it would be if  $A_1/A_t$  had been larger. This causes a small loss in thrust and specific impulse. The theory of this loss is given in Ref. 3-7.

**TABLE 3-2.** Estimated Losses for Small-Diameter Chambers

Chamber-to-Throat Area Ratio	Throat Pressure (%)	Thrust Reduction (%)	Specific Impulse Reduction (%)
$\infty$	100	0	0
3.5	99	1.5	0.31
2.0	96	5.0	0.55
1.0	81	19.5	1.34

$k = 1.20$ ;  $p_1/p_2 = 1000$ .

### 3.4. NOZZLE CONFIGURATIONS

A number of different proven nozzle configurations are available today. This section describes their geometries and performance. Other chapters (6, 8, 11, 14, and 16) discuss their materials, heat transfer, or application, and mention their requirements, design, construction, and thrust vector control. Nozzles and chambers are usually of circular cross section and have a converging section, a throat at the narrowest location (minimum cross section), and a diverging section. Nozzles can be seen in Figs. 1-4, 1-5, 1-8, 2-1, 3-11 to 3-13, 3-15, 10-2 to 10-5, 10-16, 11-1 to 11-3, and 14-6 to 14-8. Refs. 3-5 and 3-8 describe many nozzle configurations.

The *converging nozzle section* between the chamber and the nozzle throat has never been critical in achieving high performance. The subsonic flow in this section can easily be turned at very low pressure drop and any radius, cone angle, wall contour curve, or nozzle inlet shape is satisfactory. A few small attitude control thrust chambers have had their nozzle at 90 degrees from the combustion chamber axis without any performance loss. The *throat contour* also is not very critical to performance, and any radius or other curve is usually acceptable. The pressure gradients are high in these two regions and the flow will adhere to the walls. The principal difference in the different nozzle configurations is found in the diverging supersonic-flow section, as described below. The wall surface throughout the nozzle should be smooth and shiny to minimize friction, radiation absorption, and convective heat transfer due to surface roughness. Gaps, holes, sharp edges, or protrusions must be avoided.

Six different nozzle configurations are shown in Fig. 3-12 and each will be discussed. The first three sketches show conical and bell-shaped nozzles. The other three have a center body inside the nozzle and have excellent altitude compensation. Although these last three have been ground tested, to date none of them has flown in a space launch vehicle. The lengths of several nozzle types are compared in Fig. 3-13. The objectives of a good nozzle configuration are to obtain the highest practical  $I_{sp}$ , minimize inert nozzle mass, and conserve length

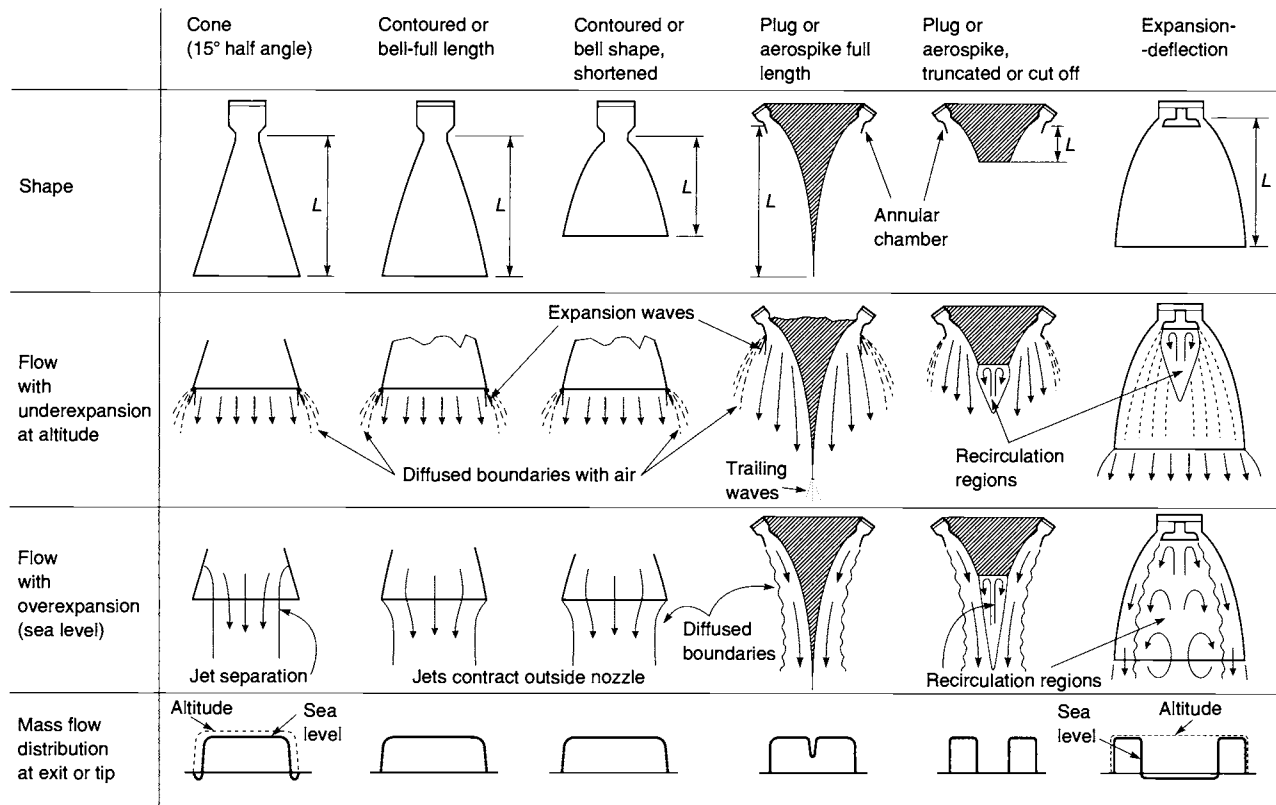


**FIGURE 3-12.** Simplified diagrams of several different nozzle configurations and their flow effects.



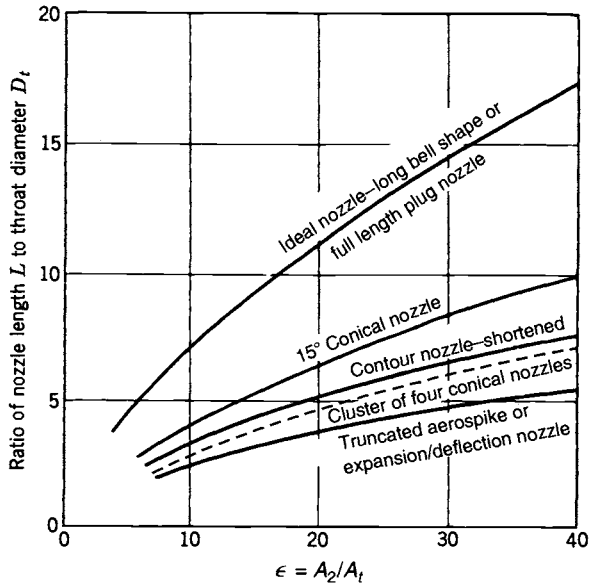


**FIGURE 3-13.** Length comparison of several types of nozzles. (Taken in part from G. V. R. Rao, "Recent Developments in Rocket Nozzle Configurations," American Rocket Society Journal, Vol. 31, No. 11, November 1961.)

(shorter nozzles can reduce vehicle length, vehicle structure, and vehicle inert mass).

### Cone- and Bell-Shaped Nozzles

The *conical nozzle* is the oldest and perhaps the simplest configuration. It is relatively easy to fabricate and is still used today in many small nozzles. A theoretical correction factor  $\lambda$  can be applied to the nozzle exit momentum of an ideal rocket with a conical nozzle exhaust. This factor is the ratio between the momentum of the gases in a nozzle with a finite nozzle angle  $2\alpha$  and the momentum of an ideal nozzle with all gases flowing in an axial direction:

$$\lambda = \frac{1}{2}(1 + \cos \alpha) \quad (3-34)$$

The variation of  $\lambda$  with different values of  $\alpha$  is shown in Table 3-3 for any nozzle that has uniform mass flow per unit exit area. For ideal rockets  $\lambda = 1.0$ . For a rocket nozzle with a divergence cone angle of  $30^\circ$  (half angle  $\alpha = 15^\circ$ ), the exit momentum and therefore the exhaust velocity will be 98.3% of the velocity calculated by Eq. 3-15b. Note that the correction factor  $\lambda$  only applies

**TABLE 3-3.** Nozzle Angle Correction Factor for Conical Nozzles

Nozzle Cone Divergence Half Angle, $\alpha$ (deg)	Correction Factor, $\lambda$
0	1.0000
2	0.9997
4	0.9988
6	0.9972
8	0.9951
10	0.9924
12	0.9890
14	0.9851
15	0.9830
16	0.9806
18	0.9755
20	0.9698
22	0.9636
24	0.9567

to the first term (the momentum thrust) in Eqs. 2-14, 3-29, and 3-30 and not to the second term (pressure thrust).

A small nozzle divergence angle causes most of the momentum to be axial and thus gives a high specific impulse, but the long nozzle has a penalty in rocket propulsion system mass, vehicle mass, and also design complexity. A large divergence angle gives short, lightweight designs, but the performance is low. There is an optimum conical nozzle shape and length (typically between 12 and 18 degrees half angle) and it is usually a compromise which depends on the specific application and flight path.

The *bell-shaped* or *contour nozzle* (see Figs. 3-12 and 3-13) is probably the most common nozzle shape today. It has a high angle expansion section (20 to 50°) right behind the nozzle throat; this is followed by a gradual reversal of nozzle contour slope so that at the nozzle exit the divergence angle is small, usually less than a 10° half angle. It is possible to go to large divergence angles immediately behind the throat (20 to 50°) because the high relative pressure, the large pressure gradient, and the rapid expansion of the working fluid do not allow separation in this region unless there are discontinuities in the nozzle contour. The expansion in the supersonic bell nozzle is more efficient than in a simple straight cone of similar area ratio and length, because the wall contour is designed to minimize losses, as explained later in this section. For the past several decades most of the nozzles have been bell shaped.

A change of flow direction of a supersonic gas in an expanding wall geometry can only be achieved through expansion waves. An expansion wave occurs at a thin surface, where the flow velocity increases and changes its flow direction slightly, and where the pressure and temperature drop. These

wave surfaces are at an oblique angle to the flow. As the gas passes through the throat, it undergoes a series of these expansion waves with essentially no loss of energy. In the bell-shaped nozzle shown in Fig. 3-14 these expansions occur internally in the flow between the throat and the inflection location  $I$ ; the area is steadily increasing like a flare on a trumpet. The contour angle  $\theta_i$  is a maximum at the inflection location. Between the inflection point  $I$  and the nozzle exit  $E$  the flow area is still increasing, but at a diminishing rate, allowing further gas expansion and additional expansion waves. However, the contour of the nozzle wall is different and the change in cross-sectional area per unit length is decreasing. The purpose of this last segment of the contoured nozzle is to have a low divergence loss as the gas leaves the nozzle exit plane. The angle at the exit  $\theta_e$  is small, usually less than  $10^\circ$ . The difference between  $\theta_i$  and  $\theta_e$  is called the turn-back angle. When the gas flow is turned in the opposite direction (between points  $I$  and  $E$ ) oblique compression waves will occur. These compression waves are thin surfaces where the flow undergoes a mild shock, the flow is turned, and the velocity is actually reduced slightly. Each of these multiple compression waves causes a small energy loss. By carefully determining the wall contour (by an analysis that uses a mathematical tool called the method of characteristics), it is possible to balance the oblique expansion waves with the oblique compression waves and minimize the energy loss. The analysis leading to the nozzle contour is presented in Chapter 20.33 of Ref. 3-3 and also in Refs. 3-8 to 3-11; it is based on supersonic aerodynamic flow, the method of characteristics (Ref. 3-1), and the properties of the expanding gas. Most of the rocket organizations have computer codes for this analysis. The radius of curvature or the contour shape at the throat region have an influence on the contour of the diverging bell-shaped nozzle section.

The length of a bell nozzle is usually given a fraction of the length of a reference conical nozzle with a  $15^\circ$  half angle. An 80% bell nozzle has a length (distance between throat plane and exit plane) that is 20% shorter than a comparable  $15^\circ$  cone of the same area ratio. Ref. 3-9 shows the original presentation by Rao of the method of characteristics applied to shorter bell nozzles. He also determined that a parabola was a good approximation for the bell-shaped contour curve (Ref. 3-3, Section 20.33), and parabolas have actually been used in some nozzle designs. The top part of Fig. 3-14 shows that the parabola is tangent ( $\theta_i$ ) at point  $I$  and has an exit angle ( $\theta_e$ ) at point  $E$  and a length  $L$  that has to be corrected for the curve  $TI$ . These conditions allow the parabola to be determined by simple geometric analysis or geometric drawing. A throat approach radius of  $1.5 r_t$  and a throat expansion radius of  $0.4 r_t$  were used. If somewhat different radii had been used, the results would have been only slightly different. The middle set of curves gives the relation between length, area ratio, and the two angles of the bell contour. The bottom set of curves gives the correction factors, equivalent to the  $\lambda$  factor for conical nozzles, which are to be applied to the thrust coefficient or the exhaust velocity, provided the nozzles are at optimum expansions, that is,  $p_2 = p_3$ .

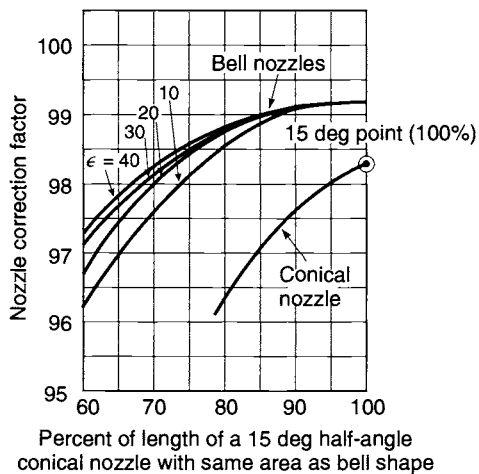
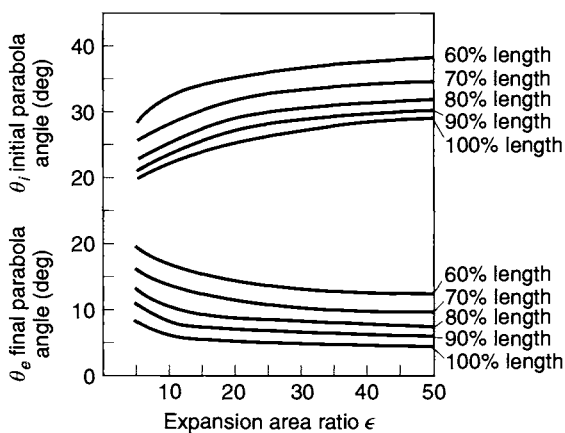
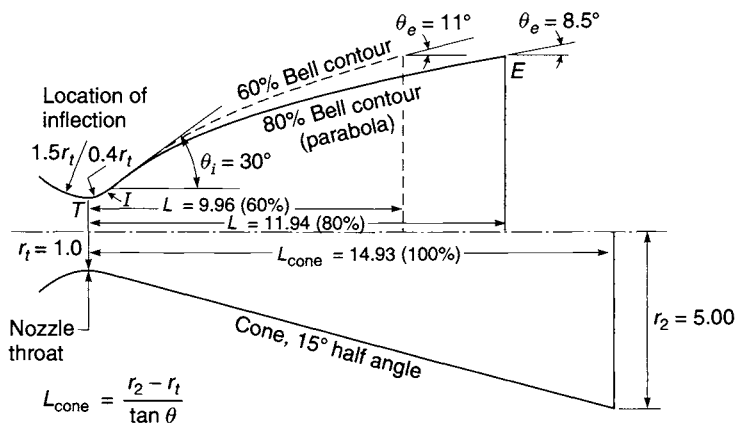


**TABLE 3-4.** Data on Several Bell-Shaped Nozzles

Area Ratio	10	25	50
<i>Cone (15° Half Angle)</i>			
Length (100%) <sup>a</sup>	8.07	14.93	22.66
Correction factor $\lambda$	0.9829	0.9829	0.9829
<i>80% Bell Contour</i>			
Length <sup>a</sup>	6.45	11.94	18.12
Correction factor $\lambda$	0.985	0.987	0.988
Approximate half angle at inflection point and exit (degrees)	25/10	30/8	32/7.5
<i>60% Bell Contour</i>			
Length <sup>a</sup>	4.84	9.96	13.59
Correction factor $\lambda$	0.961	0.968	0.974
Approximate half angle at inflection point and exit (degrees)	32.5/17	36/14	39/18

<sup>a</sup>The length is given in dimensionless form as a multiple of the throat radius, which is one.

Table 3-4 shows data for parabolas developed from this figure, which allow the reader to apply this method and check the results. The table shows two shortened bell nozzles and a conical nozzle, each for three area ratios. It can be seen that as the length has been decreased, the losses are higher for the shorter length and slightly higher for small nozzle area ratios. A 1% improvement in the correction factor gives about 1% more specific impulse (or thrust) and this difference can be significant in many applications. The reduced length is an important benefit, and it is usually reflected in an improvement of the vehicle mass ratio. The table and Fig. 3-14 show that bell nozzles (75 to 85% length) are just as efficient as or slightly more efficient than a longer 15° conical nozzle (100% length) at the same area ratio. For shorter nozzles (below 70% equivalent length) the energy losses due to internal oblique shock waves become substantial and such short nozzles are not commonly used today.

For solid propellant rocket motor exhausts with small solid particles in the gas (usually aluminum oxide), and for exhausts of certain gelled liquid propellants, there is an impingement of these solid particles against the nozzle wall in

**FIGURE 3-14.** Top sketch shows comparison sketches of nozzle inner wall surfaces for a 15° conical nozzle, an 80% length bell nozzle, a 60% length bell nozzle, all at an area ratio of 25. The lengths are expressed in multiples of the throat radius  $r_t$ , which is one here. The middle set of curves shows the initial angle  $\theta_i$  and the exit angle  $\theta_e$  as functions of the nozzle area ratio and percent length. The bottom curves show the nozzle losses in terms of a correction factor. Adapted and copied with permission of AIAA from Ref. 6-1.

the reversing curvature section between  $I$  and  $E$  in Fig. 3-14. While the gas can be turned by oblique waves to have less divergence, the particles (particularly the larger particles) have a tendency to move in straight lines and hit the walls at high velocity. The resulting abrasion and erosion of the nozzle wall can be severe, especially with the ablative and graphite materials that are commonly used. This abrasion by hot particles increases with turn-back angle. If the turn-back angle and thus also the inflection angle  $\theta_i$  are reduced, the erosion can become acceptable. Typical solid rocket motors flying today have values of inflection angles between 20 and 26° and turn-back angles of 10 to 15°. In comparison, current liquid rocket engines without entrained particles have inflection angles between 27 and 50° and turn-back angles of between 15 and 30°. Therefore the performance enhancement caused by using a bell-shaped nozzle (high value of correction factor) is somewhat lower in solid rocket motors with solid particles in the exhaust.

The ideal bell-shaped nozzle (minimum loss) is long, equivalent to a conical nozzle of perhaps 10 to 12°, as seen in Fig. 3-12. It has about the same length as a full-length aerospike nozzle. This is usually too long for reasonable vehicle mass ratios.

**Two-Step Nozzles.** Several modifications of a bell-shaped nozzle have evolved that allow full or almost complete altitude compensation; that is, they achieve maximum performance at more than a single altitude. Figure 3-15 shows three concepts for a two-step nozzle, one that has an initial low area ratio  $A_2/A_1$  for operation at or near the earth's surface and a larger second area ratio that improves performance at high altitudes. See Ref. 3-5.

The *extendible nozzle* requires actuators, a power supply, mechanisms for moving the extension into position during flight, fastening and sealing devices. It has successfully flown in several solid rocket motor nozzles and in a few liquid engine applications, where it was deployed prior to ignition. Although only two steps are shown, there have been versions with three steps; one is shown in Fig. 11-3. As yet it has not made the change in area ratio during rocket firing. The principal concerns are a reliable rugged mechanism to move the extension into position, the hot gas seal between the nozzle sections, and the extra weight involved.

The *droppable insert concept* avoids the moving mechanism and gas seal but has a potential stagnation temperature problem at the joint. It requires a reliable release mechanism, and the ejected insert creates flying debris. To date it has little actual test experience. See Ref. 3-12.

The *dual bell nozzle concept* uses two shortened bell nozzles combined into one with a bump or inflection point between them, as shown in Fig. 3-15. During ascent it functions first at the lower area ratio, with separation occurring at the inflection point. As altitude increases and the gas expands further, the flow attaches itself downstream of this point, with the flow filling the full nozzle exit section and operating with the higher area ratio at higher performance. There is a small performance penalty for a compromised bell nozzle

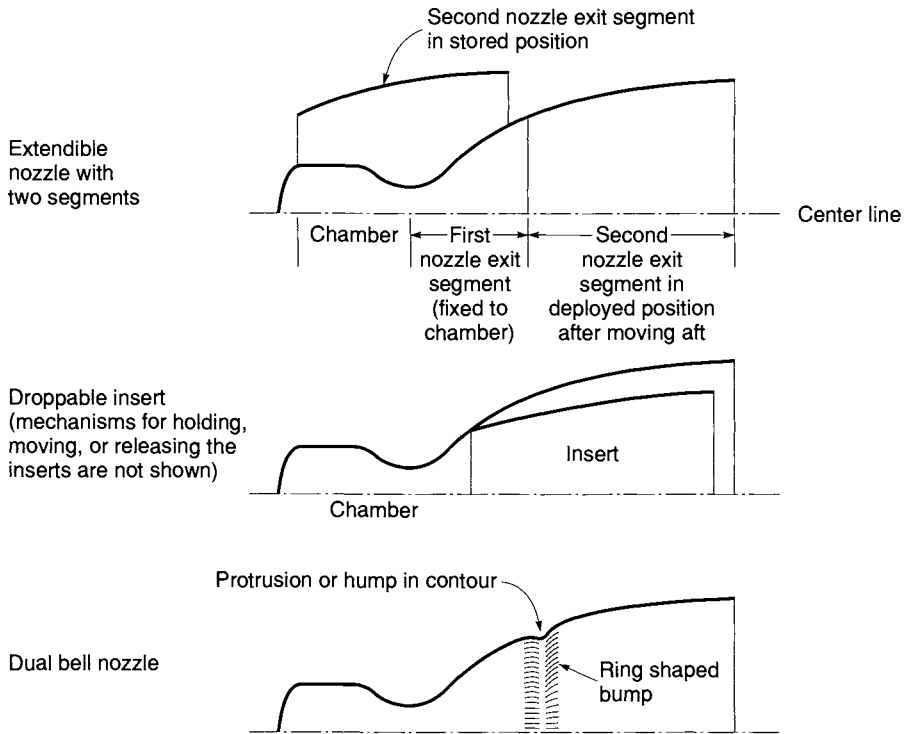


**FIGURE 3-15.** Simplified diagrams of three altitude-compensating two-step nozzle concepts.

contour with a circular bump. To date there has been little experience with this concept.

### Nozzles with Aerodynamic Boundaries

The group of two-step nozzle concepts described above corresponds to the performance represented by upper portions of the two fixed area ratio nozzle curves shown in Fig. 3-10; the performance of a continuously varying nozzle with full altitude compensation is shown by the dashed curve. When integrated over the flight time, the extra performance is important for high velocity missions such as the single stage to orbit application. The three nozzles shown on the right side of Fig. 3-12 offer full altitude compensation and are discussed next. Refs. 3-5 and 3-8 give more information.

The *plug nozzle* or *aerospike nozzle* has an annular doughnut-shaped chamber with an annular nozzle slot. An alternate version has a number of individual small chambers (each with low area ratio short nozzles, a round throat, and a rectangular exit) arranged in a circle around a common plug or spike. The outside aerodynamic boundary of the gas flow in the divergent section of

the nozzle is the interface between the hot gas and the ambient air; there is no outer wall as in a conical or bell-shaped nozzle. As the external or ambient pressure is reduced during the ascending flight, this gas boundary expands outward, causes a change in pressure distribution on the central spike, and allows an automatic and continuous altitude compensation. The aerospike contour with the minimum flow losses turns out to be very long, similar in length to an optimum bell nozzle as shown in Figs. 3-12 and 3-13. The mass flow per unit exit area is relatively uniform over the cross section and the divergence losses are minimal.

If the central plug is cut off or truncated and the wall contour is slightly altered, then the nozzle will be very short, as shown in Fig. 3-13; it will have some internal supersonic waves and will show a small but real loss in thrust compared to a nozzle with a full central spike. The pressure distribution and the heat transfer intensity vary on the inner contoured spike wall surface. Figure 8-14 shows a typical pressure distribution over the contoured spike surface at high and low altitudes.

The pressure in the recirculating trapped gas of the subsonic region below the bottom plate also exerts a thrust force. The losses caused by the cut-off spike can be largely offset by injecting a small amount of the gas flow (about 1% of total flow) through this base plate into the recirculating region, thus enhancing the back pressure on the base plate. The advantages of the truncated aerospike are short length (which helps to reduce the length and mass of the flight vehicle), full altitude compensation, no flow separation from the wall at lower altitudes, and ease of vehicle/engine integration for certain vehicle configurations.

The *linear aerospike nozzle* is a variation of the round axisymmetric aerospike nozzle. Basically, it is an unrolled version of the circular configuration. It is explained further in Chapter 8.2.

In the *expansion deflection nozzle* (Fig. 3-12) the flow from the chamber is directed radially outward away from the nozzle axis. The flow is turned on a curved contour outer diverging nozzle wall. The nozzle has been shortened and has some internal oblique shock wave losses. The hot gas flow leaving the chamber expands around a central plug. The aerodynamic interface between the ambient air and gas flow forms an inner boundary of the gas flow in the diverging nozzle section. As the ambient pressure is reduced, the hot gas flow fills more and more of the nozzle diverging section. Altitude compensation is achieved by this change in flow boundary and by changes in the pressure distribution on the outer walls.

**Multiple Nozzles.** If a single large nozzle is replaced by a cluster of smaller nozzles on a solid motor (all at the same cumulative thrust), then it is possible to reduce the nozzle length. Similarly, if a single large thrust chamber of a liquid engine is replaced by several smaller thrust chambers, the nozzle length will be shorter, reducing the vehicle length and thus the vehicle structure and inert mass. Russia has pioneered a set of four thrust chambers, each with 25%



of the total thrust, assembled next to each other and fed from the same liquid propellant feed system. This quadruple thrust chamber arrangement has been used effectively on many large Russian space launch vehicles and missiles. As seen in Fig. 3-13, this cluster is about 30% shorter than a single large thrust chamber. The vehicle diameter at the cluster nozzle exit is somewhat larger, the vehicle drag is somewhat higher, and there is additional engine complexity and engine mass.

### 3.5. REAL NOZZLES

In a real nozzle the flow is really two-dimensional, but axisymmetric. For simple single nozzle shapes the temperatures and velocities are not uniform over any one section and are usually higher in the central region and lower near the periphery. For example, the surface where the Mach number is one is a plane at the throat for an ideal nozzle; for two-dimensional flow it is typically a slightly curved surface somewhat downstream of the throat. If the velocity distribution is known, the average value of  $v_2$  can be determined for an axisymmetric nozzle as a function of the radius  $r$ .

$$(v_2)_{\text{average}} = \frac{2\pi}{A_2} \int_0^{r_2} v_2 r \, dr \quad (3-35)$$

The 11 assumptions and simplifications listed in Section 1 of this chapter are only approximations that allow relatively simple algorithms and simple mathematical solutions to the analysis of real rocket nozzle phenomena. For most of these assumptions it is possible either (1) to use an empirical correction factor (based on experimental data) or (2) to develop or use a more accurate algorithm, which involves more detailed understanding and simulation of energy losses, the physical or chemical phenomena, and also often a more complex theoretical analysis and mathematical treatment. Some of these approaches are mentioned briefly in this section.

Compared to an ideal nozzle, the real nozzle has energy losses and energy that is unavailable for conversion into kinetic energy of the exhaust gas. The principal losses are listed below and several of these are discussed in more detail.

1. The *divergence of the flow* in the nozzle exit sections causes a loss, which varies as a function of the cosine of the divergence angle as shown by Eq. 3-34 and Table 3-3 for conical nozzles. The losses can be reduced for bell-shaped nozzle contours.
2. Small chamber or port area cross sections relative to the throat area or *low nozzle contraction ratios*  $A_1/A_t$  cause pressure losses in the chamber and reduce the thrust and exhaust velocity slightly. See Table 3-2.

3. Lower flow velocity in the *boundary layer* or wall friction can reduce the effective exhaust velocity by 0.5 to 1.5%.
4. *Solid particles* or *liquid roplets* in the gas can cause losses up to 5%, as described below.
5. *Unsteady combustion* and oscillating flow can account for a small loss.
6. *Chemical reactions in nozzle flow* change gas properties and gas temperatures, giving typically a 0.5% loss. See Chapter 5.
7. There is lower performance during *transient pressure operation*, for example during start, stop, or pulsing.
8. For uncooled nozzle materials, such as fiber reinforced plastics or carbon, the gradual *erosion* of the *throat region* increases the throat diameter by perhaps 1 to 6% during operation. In turn this will reduce the chamber pressure and thrust by about 1 to 6% near the end of the operation and cause a slight reduction in specific impulse of less than 0.7%.
9. *Non-uniform gas composition* can reduce performance (due to incomplete mixing, turbulence, or incomplete combustion regions).
10. Using *real gas properties* can at times change the gas composition, the value of  $k$  and  $\mathfrak{M}$ , and this can cause a small loss in performance, say 0.2 to 0.7%.
11. Operation at non-optimum nozzle expansion area ratio can reduce thrust and specific impulse. There is no loss if the vehicle always flies at the altitude for optimum nozzle expansion ( $p_2 = p_3$ ). If it flies with a fixed nozzle area ratio at higher or lower altitudes, then there is a loss (during a portion of the flight) by up to 15% in thrust compared to a nozzle with altitude compensation, as can be seen in Figs. 3-7 and 3-8. It also reduces performance by 1 to 5%.

## Boundary Layer

Real nozzles have a viscous *boundary layer* next to the nozzle walls, where the gas velocities are much lower than the free-stream velocities in the inviscid flow regions. An enlarged schematic view of a boundary layer is shown in Fig. 3-16. Immediately next to the wall the flow velocity is zero and then the boundary layer can be considered as being built up of successive annular-shaped thin layers of increasing velocity until the free-stream velocity is reached. The low-velocity flow close to the wall is laminar and subsonic, but in the higher-velocity regions of the boundary layer the flow is supersonic and can become turbulent. The local temperature in part of the boundary layer can be substantially higher than the free-stream temperature because of the conversion of kinetic energy into thermal energy as the local velocity is slowed down and as heat is created by viscous friction. The layer right next to the wall will be cooler because of heat transfer to the wall. The gaseous

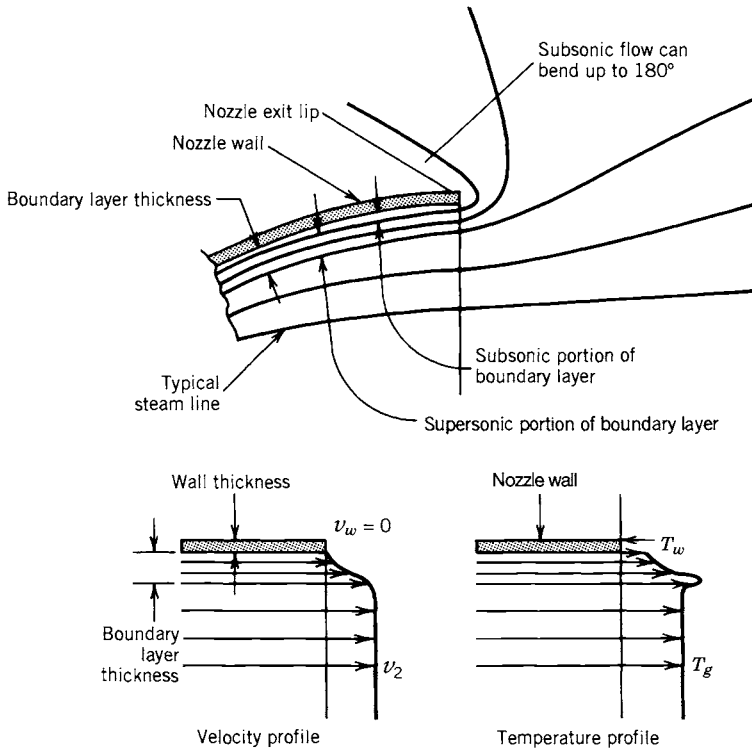


**FIGURE 3-16.** Flow conditions at a nozzle exit lip at high altitude, showing streamlines, boundary layer, velocity and temperature profiles.

boundary layer has a profound effect on the overall heat transfer to nozzle and chamber walls. It also has an effect on the rocket performance, particularly in applications with relatively long nozzles with high nozzle area ratios, where a relatively high proportion of the total mass flow (2 to 25%) can be in the lower-velocity region of the boundary layer. The high gradients in pressure, temperature, or density and the changes in local velocity (direction and magnitude) influence the boundary layer. Scaling laws for boundary layer phenomena have not been reliable.

Theoretical approaches to boundary layer performance effects can be found in Chapters 26 to 28 of Reference 3-1 and in Reference 1-1. A truly satisfactory theoretical analysis of boundary layers in rocket nozzles has not yet been developed. Fortunately, the overall effect of boundary layers on rocket performance has been small. For most rocket nozzles the loss seldom exceeds 1% of specific impulse.

## Multiphase Flow

In some rockets the gaseous working fluid contains many small liquid droplets and/or solid particles that must be accelerated by the gas. They give up heat to the gas during the expansion in a nozzle. This, for example, occurs with solid propellants (see Chapter 12) or some gelled liquid propellants (Chapter 7), which contain aluminum powder that forms small oxide particles in the exhaust. It can also occur with ion oxide catalysts, or propellants containing beryllium, boron, or zirconium.

In general, if the particles are very small (typically with diameters of 0.005 mm or less), they will have almost the same velocity as the gas and will be in thermal equilibrium with the nozzle gas flow. Thus, as the gases give up kinetic energy to accelerate the particles, they gain thermal energy from the particles. As the particle diameters become larger, the mass (and thus the inertia) of the particle increases as the cube of its diameter; however, the drag force increases only as the square of the diameter. Larger particles therefore do not move as fast as the gas and do not give heat to the gas as readily as do smaller particles. The larger particles have a lower momentum than an equivalent mass of smaller particles and they reach the nozzle exit at a higher temperature than the smaller particles, thus giving up less thermal energy.

It is possible to derive a simple theoretical approach for correcting the performance ( $I_s$ ,  $c$ , or  $c^*$ ) as shown below and as given in Refs. 3-13 and 3-14. It is based on the assumption that specific heats of the gases and the particles are constant throughout the nozzle flow, that the particles are small enough to move at the same velocity as the gas and are in thermal equilibrium with the gas, and that particles do not exchange mass with the gas (no vaporization or condensation). Expansion and acceleration occur only in the gas and the volume occupied by the particles is negligibly small compared to the gas volume. If the amount of particles is small, the energy needed to accelerate the particles can be neglected. There are no chemical reactions.

The enthalpy  $h$ , the specific volume  $V$ , and the gas constant  $R$  can be expressed as functions of the particle fraction  $\beta$ , which is the mass of particles (liquid and/or solid) divided by the total mass. Using the subscripts  $g$  and  $s$  to refer to the gas or solid state, the following relationships then apply:

$$h = (1 - \beta)(c_p)_g T + \beta c_s T \quad (3-36)$$

$$V = V_g(1 - \beta) \quad (3-37)$$

$$p = R_g T / V_g \quad (3-38)$$

$$R = (1 - \beta)R_g \quad (3-39)$$

$$k = \frac{(1 - \beta)c_p + \beta c_s}{(1 - \beta)c_v + \beta c_s} \quad (3-40)$$

These relations are then used in the formulas for simple one-dimensional nozzle flow, such as Eq. 2-16, 3-15, or 3-32. The values of specific impulse or

characteristic velocity will decrease as  $\beta$ , the percent of particles, is increased. For very small particles (less than 0.01 mm in diameter) and small values of  $\beta$  (less than 6%) the loss in specific impulse is often less than 2%. For larger particles (over 0.015 mm diameter) and larger values of  $\beta$  this theory is not helpful and the specific impulse can be 10 to 20% less than the  $I_s$  value without flow lag. The actual particle sizes and distribution depend on the specific propellant, the combustion, the particular particle material, and the specific rocket propulsion system, and usually have to be measured (see Chapters 12 and 18). Thus adding a metal, such as aluminum, to a solid propellant will increase the performance only if the additional heat release can increase the combustion temperature  $T_1$  sufficiently so that it more than offsets the decrease caused by particles in the exhaust.

With very-high-area-ratio nozzles and a low nozzle exit pressure (high altitude or space vacuum) it is possible to condense some of the propellant ingredients that are normally gases. As the temperature drops sharply in the nozzle, it is possible to condense gaseous species such as  $\text{H}_2\text{O}$ ,  $\text{CO}_2$ , or  $\text{NH}_3$  and form liquid droplets. This causes a decrease in the gas flow per unit area and the transfer of the latent heat of vaporization to the remaining gas. The overall effect on performance is small if the droplet size is small and the percent of condensed gas mass is moderate. It is also possible to form a solid phase and precipitate fine particles of snow ( $\text{H}_2\text{O}$ ) or frozen fog of other species.

### Other Phenomena and Losses

The *combustion process* is really not steady. Low- and high-frequency oscillations in chamber pressure of up to perhaps 5% of rated value are usually considered as smooth-burning and relatively steady flow. Gas properties ( $k$ ,  $\mathfrak{M}$ ,  $c_p$ ) and flow properties ( $v$ ,  $V$ ,  $T$ ,  $p$ , etc.) will also oscillate with time and will not necessarily be uniform across the flow channel. These properties are therefore only “average” values, but it is not always clear what kind of an average they are. The energy loss due to nonuniform unsteady burning is difficult to assess theoretically. For smooth-burning rocket systems they are negligibly small, but they become significant for larger-amplitude oscillations.

The *composition of the gas* changes somewhat in the nozzle, chemical reactions occur in the flowing gas, and the assumption of a uniform or “frozen” equilibrium gas composition is not fully valid. A more sophisticated analysis for determining performance with changing composition and changing gas properties is described in Chapter 5. The thermal energy that is carried out of the nozzle ( $\dot{m} c_p T_2$ ) is unavailable for conversion to useful propulsive (kinetic) energy, as is shown in Fig. 2-3. The only way to decrease this loss is to reduce the nozzle exit temperature  $T_2$  (larger nozzle area ratio), but even then it is a large loss.

When the operating durations are short (as, for example, with antitank rockets or pulsed attitude control rockets which start and stop repeatedly), the start and stop *transients* are a significant portion of the total operating

time. During the transient periods of start and stop the average thrust, chamber pressure, or specific impulse will be lower in value than those same parameters at steady full operating conditions. This can be analyzed in a step-by-step process. For example, during startup the amount of propellant reacting in the chamber has to equal the flow of gas through the nozzle plus the amount of gas needed to fill the chamber to a higher pressure; alternatively, an empirical curve of chamber pressure versus time can be used as the basis of such a calculation. The transition time is very short in small, low-thrust propulsion systems, perhaps a few milliseconds, but it can be longer (several seconds) for large propulsion systems.

### Performance Correction Factors

In this section we discuss semiempirical correction factors that have been used to estimate the test performance data from theoretical, calculated performance values. An understanding of the theoretical basis also allows correlations between several of the correction factors and estimates of the influence of several parameters, such as pressure, temperature, or specific heat ratio.

The *energy conversion efficiency* is defined as the ratio of the kinetic energy per unit of flow of the actual jet leaving the nozzle to the kinetic energy per unit of flow of a hypothetical ideal exhaust jet that is supplied with the same working substance at the same initial state and velocity and expands to the same exit pressure as the real nozzle. This relationship is expressed as

$$e = \frac{(v_2)_a^2}{(v_2)_i^2} = \frac{(v_2)_a^2}{(v_1)_a^2 + c_p(T_1 - T_2)} \quad (3-41)$$

where  $e$  denotes the energy conversion efficiency,  $v_1$  and  $v_2$  the velocities at the nozzle inlet and exit, and  $c_p T_1$  and  $c_p T_2$  the respective enthalpies for an ideal isentropic expansion. The subscripts  $a$  and  $i$  refer to actual and ideal conditions, respectively. For many practical applications,  $v_1 \rightarrow 0$  and the square of the expression given in Eq. 3-16 can be used for the denominator.

The *velocity correction factor*  $\zeta_v$  is defined as the square root of the energy conversion efficiency  $\sqrt{e}$ . Its value ranges between 0.85 and 0.99, with an average near 0.92. This factor is also approximately the ratio of the actual specific impulse to the ideal or theoretical specific impulse.

The *discharge correction factor*  $\zeta_d$  is defined as the ratio of the mass flow rate in a real rocket to that of an ideal rocket that expands an identical working fluid from the same initial conditions to the same exit pressure (Eq. 2-17).

$$\zeta_d = (\dot{m}_a/\dot{m}_i) = \dot{m}_a(c/F_i) \quad (3-42)$$

and, from Eq. 3-24,

$$\zeta_d = \frac{\dot{m}_a \sqrt{kRT_1}}{A_t p_1 k \sqrt{[2/(k+1)]^{(k+1)/(k-1)}}}$$

The value of this discharge correction factor is usually larger than 1 (1.0 to 1.15); the actual flow is larger than the theoretical flow for the following reasons:

1. The molecular weight of the gases usually increases slightly when flowing through a nozzle, thereby changing the gas density.
2. Some heat is transferred to the nozzle walls. This lowers the temperature in the nozzle, and increases the density and mass flow slightly.
3. The specific heat and other gas properties change in an actual nozzle in such a manner as to slightly increase the value of the discharge correction factor.
4. Incomplete combustion can increase the density of the exhaust gases.

The actual thrust is usually lower than the thrust calculated for an ideal rocket and can be found by an empirical *thrust correction* factor  $\zeta_F$ :

$$F_a = \zeta_F F_i = \zeta_F C_F p_1 A_t = \zeta_F c_i \dot{m}_i \quad (3-43)$$

where

$$\zeta_F = \zeta_v \zeta_d = F_a / F_i \quad (3-44)$$

Values of  $\zeta_F$  fall between 0.92 and 1.00 (see Eqs. 2-6 and 3-31). Because the thrust correction factor is equal to the product of the discharge correction factor and the velocity correction factor, any one can be determined if the other two are known.

**Example 3-7.** Design a rocket nozzle to conform to the following conditions:

Chamber pressure	20.4 atm = 2.068 MPa
Atmospheric pressure	1.0 atm
Chamber temperature	2861 K
Mean molecular mass of gases	21.87 kg/kg-mol
Ideal specific impulse	230 sec (at operating conditions)
Specific heat ratio	1.229
Desired thrust	1300 N

Determine the following: nozzle throat and exit areas, respective diameters, actual exhaust velocity, and actual specific impulse.

**SOLUTION.** The theoretical thrust coefficient is found from Eq. 3-30. For optimum conditions  $p_2 = p_3$ . By substituting  $k = 1.229$  and  $p_1/p_2 = 20.4$ , the thrust coefficient is  $C_F = 1.405$ . This value can be checked by interpolation between the values of  $C_F$

obtained from Figs. 3-7 and 3-8. The throat area is found using  $\zeta_F = 0.96$ , which is based on test data.

$$A_t = F/(\zeta_F C_F p_1) = 1300/(0.96 \times 1.405 \times 2.068 \times 10^6) = 4.66 \text{ cm}^2$$

The throat diameter is then 2.43 cm. The area expansion ratio can be determined from Fig. 3-5 or Eq. 3-25 as  $\epsilon = 3.42$ . The exit area is

$$A_2 = 4.66 \times 3.42 = 15.9 \text{ cm}^2$$

The exit diameter is therefore 4.50 cm. The theoretical exhaust velocity is

$$v_2 = I_s g_0 = 230 \times 9.81 = 2256 \text{ m/sec}$$

By selecting an empirical velocity correction factor  $\zeta_v$  such as 0.92 (based on prior related experience), the actual exhaust velocity will be equal to

$$(v_2)_a = 2256 \times 0.92 = 2076 \text{ m/sec}$$

Because the specific impulse is proportional to the exhaust velocity, its actual value can be found by multiplying the theoretical value by the velocity correction factor  $\zeta_v$ .

$$(I_s)_a = 230 \times 0.92 = 212 \text{ sec}$$

### 3.6. FOUR PERFORMANCE PARAMETERS

In using values of thrust, specific impulse, propellant flow, and other performance parameters, one must be careful to specify or qualify the conditions under which a specific number is presented. There are at least four sets of performance parameters and they are often quite different in concept and value, even when referring to the same rocket propulsion system. Each performance parameter, such as  $F$ ,  $I_s$ ,  $c$ ,  $v_2$  and/or  $\dot{m}$ , should be accompanied by a clear definition of the conditions under which it applies, namely:

- a. Chamber pressure; also, for slender chambers, the location where this pressure prevails (e.g., at nozzle entrance).
- b. Ambient pressure or altitude or space (vacuum).
- c. Nozzle expansion area ratio and whether this is an optimum.
- d. Nozzle shape and exit angle (see Table 3-3).
- e. Propellants, their composition or mixture ratio.
- f. Key assumptions and corrections made in the calculations of the theoretical performance: for example, was frozen or shifting equilibrium used in the analysis? (This is described in Chapter 5.)
- g. Initial temperature of propellants.



1. *Theoretical performance values* are defined in Chapters 2, 3, and 5 and generally apply to ideal rockets, but usually with some corrections. Most organizations doing nozzle design have their own computer programs, often different programs for different nozzle designs, different thrust levels, or operating durations. Most are two dimensional and correct for the chemical reactions in the nozzle using real gas properties, and correct for divergence. Many also correct for one or more of the other losses mentioned above. For example, programs for solid propellant motor nozzles can include losses for throat erosion and multiphase flow; for liquid propellant engines it may include two or more concentric zones, each at different mixtures ratios and thus with different gas properties. Nozzle wall contour analysis with expansion and compression waves may use a finite element analysis and/or a method of characteristics approach. Some of the more sophisticated programs include viscous boundary layer effects and heat transfer to the walls. Typically these computer simulation programs are based on computer fluid dynamics finite element analyses and on the basic Navier–Stokes relationships. Most companies also have simpler, one-dimensional computer programs which may include one or more of the above corrections; they are used frequently for preliminary estimates or proposals.

2. *Delivered, that is, actually measured, performance values* are obtained from static tests or flight tests of full-scale propulsion systems. Again, the conditions should be explained (e.g., define  $p_1$ ,  $A_2/A_t$ ,  $T_1$ , etc.) and the measured values should be corrected for instrument deviations, errors, or calibration constants. Flight test data need to be corrected for aerodynamic effects, such as drag. Often empirical coefficients, such as the thrust correction factor, the velocity correction factor, and the mass discharge flow correction factors are used to convert the theoretical values of item 1 above to approximate actual values and this is often satisfactory for preliminary estimates. Sometimes subscale propulsion systems are used in the development of new rocket systems and then scale factors are used to correct the measured data to full-scale values.

3. *Performance values at standard conditions* are corrected values of items 1 and 2 above. These standard conditions are generally rigidly specified by the customer. Usually they refer to conditions that allow ready evaluation or comparison with reference values and often they refer to conditions that can be easily measured and/or corrected. For example, to allow a good comparison of specific impulse for several propellants or rocket propulsion systems, the values are often corrected to the following standard conditions (see Examples 3–4 and 3–5):

- a.  $p_1 = 1000$  psia or  $6.894 \times 10^6$  Pa.
- b.  $p_2 = p_3 = 14.69$  psia (sea level) or  $1.0132 \times 10^5$  Pa or 0.10132 MPa.
- c. Area ratio is optimum,  $p_2 = p_3$ .
- d. Nozzle divergence half angle  $\alpha = 15^\circ$  for conical nozzles, or some agreed-upon value.

- e. Specific propellant, its design mixture ratio and/or propellant composition.
- f. Propellant initial temperature:  $21^{\circ}\text{C}$  (sometimes  $20$  or  $25^{\circ}\text{C}$ ) or boiling temperature, if cryogenic.

A rocket propulsion system is generally designed, built, tested, and delivered in accordance with some predetermined requirements or *specifications*, usually in formal documents often called the *rocket engine or rocket motor specifications*. They define the performance as shown above and they also define many other requirements. More discussion of these specifications is given as a part of the selection process for propulsion systems in Chapter 17.

4. Rocket manufacturers are often required by their customers to deliver rocket propulsion systems with a *guaranteed minimum performance*, such as minimum  $F$  or  $I_s$  or both. The determination of this value can be based on a nominal value (items 1 or 2 above) diminished by all likely losses, including changes in chamber pressure due to variation of pressure drops in injector or pipelines, a loss due to nozzle surface roughness, propellant initial ambient temperatures, manufacturing variations from rocket to rocket (e.g., in grain volume, nozzle dimensions, or pump impeller diameters, etc.). This minimum value can be determined by a probabilistic evaluation of these losses and is then usually validated by actual full-scale static and flights tests.

### 3.7. NOZZLE ALIGNMENT

When the thrust line or direction does not intersect the center of mass of a flying vehicle, a turning moment will tend to rotate a vehicle in flight. Turning moments are desirable and necessary for the controlled turning or attitude control of a vehicle as is routinely done by means of the deflection of the thrust vector, aerodynamic fins, or by separate attitude control rocket engines. However, this turning is undesirable when its magnitude or direction is not known; this happens when a fixed nozzle of a major propulsion system has its thrust axis misaligned. A large high-thrust booster rocket system, even if misaligned by a very small angle (less than  $\frac{1}{2}^{\circ}$ ), can cause major upsetting turning moments for the firing duration. If not corrected or compensated, such a small misalignment can cause the flight vehicle to tumble and/or deviate from the intended flight path. For this moment not to exceed the vehicle's compensating attitude control capability, it is necessary to align the nozzle axis of all propulsion systems with fixed (non-gimbal) nozzles very accurately. Normally, the geometric axis of the nozzle diverging exit surface geometry is taken to be the thrust axis. Special alignment fixtures are usually needed to orient the nozzle axis to be within less than  $\pm 0.25^{\circ}$  of the intended line to the vehicle's center of gravity and to position the center of a large

nozzle throat to be on the vehicle centerline, say within 1 or 2 mm. See Ref. 3-15.

There are other types of misalignments: (1) irregularities in the nozzle geometry (out of round, protuberances, or unsymmetrical roughness in the surface); (2) transient misalignments during start to stop; (3) uneven deflection of the propulsion system or vehicle structure under load; and (4) irregularities in the gas flow (faulty injector, uneven burning rate in solid propellants). For simple unguided rocket vehicles it has been customary to rotate or spin the vehicle to prevent the misalignment from being in one direction only or to even out the misalignment during powered flight.

In the cramped volume of spacecraft or upper stage launch vehicles, it is sometimes not possible to accommodate the full length of a large-area-ratio nozzle within the available vehicle envelope. In this case the nozzles are cut off at an angle at the vehicle surface, which allows a compact installation. Figure 3-17 shows a diagram of two (out of four) roll control thrusters whose nozzle exit conforms to the vehicle contour. The thrust direction of a *scarfed* nozzle is

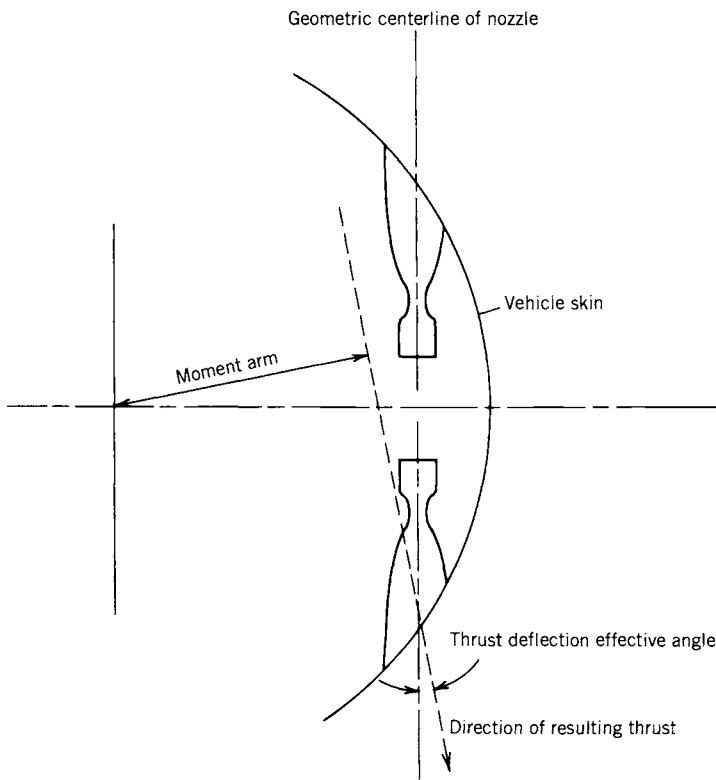


**FIGURE 3-17.** Simplified partial section of a flight vehicle showing two attitude control thrusters with scarfed nozzles to fit a cylindrical vehicle envelope.

no longer on the nozzle axis centerline, as it is with fully symmetrical nozzles, and the nozzle exit flow will not be axisymmetric. Reference 3-16 shows how to estimate the performance and thrust direction of scarfed nozzles

### 3.8. VARIABLE THRUST

Only a few applications require a change in thrust during flight. Equations 3-30, 3-24, and 3-31 show that the thrust is directly proportional to the throat area  $A_t$ , the chamber pressure  $p_1$ , or the mass flow rate  $\dot{m}$ , but it is a weak function of  $C_F$ , which in turn depends on  $k$ , the altitude, a pressure ratio, and  $A_2/A_t$ . These equations show how the thrust may be varied and imply how other performance parameters may be affected by such variation. For liquid propellant rockets the mass flow to the chamber can be decreased (by throttling valves in the propellant feed system) while the chamber geometry and the nozzle throat area are unchanged. The reduced mass flow will cause an almost linear decrease in  $p_1$  and thus an almost linear decrease of  $F$ . The combustion temperature does change slightly but it does not enter into the above relations. The specific impulse would also decrease slightly. Thus, there is a small performance penalty for throttling the thrust. A two-to-one thrust decrease has been achieved with throttle valves in a liquid propellant rocket engine. Random throttling of liquid propellant engines and their design features are discussed in Chapter 8.5.

Another way of varying the thrust is to change the throat area simultaneously with throttling the flow (by inserting a moveable contoured pintle or tapered plug into the nozzle); in this case the chamber pressure  $p_1$  can remain reasonably constant. This throttling method has been used on liquid propellant engines (e.g., a ten-to-one thrust change on a moon landing rocket) and in a few experimental solid propellant motors.

Random thrust control requires a control system and special hardware; one example is discussed in Chapter 10.5. Random throttling of production solid propellant motors has not been achieved as yet in flight. A repeatable, programmed variation of thrust for solid propellants is possible and is discussed in Chapter 11.3. For solid propellants, a predetermined variation of mass flow rate has been achieved by clever grain geometric design, which changes the burning area at different stages during the operation. This is useful in many air-launched military rockets. Liquid propellant rockets are the most appropriate choice for randomly variable thrust rockets, as has been amply demonstrated in missions such as the lunar landings.

## PROBLEMS

1. Certain experimental results indicate that the propellant gases of a liquid oxygen–gasoline reaction have a mean molecular mass of 23.2 kg/kg-mol and a specific heat ratio of 1.22. Compute the specific heat at constant pressure and at constant volume, assuming a perfect gas.
2. The actual conditions for an optimum expansion nozzle operating at sea level are given below. Calculate  $v_2$ ,  $T_2$ , and  $C_F$ . The mass flow  $\dot{m} = 3.7$  kg/sec;  $p_1 = 2.1$  MPa;  $T_1 = 2585^\circ\text{K}$ ;  $\mathfrak{M} = 18.0$  kg/kg-mol; and  $k = 1.30$ .
3. A certain nozzle expands a gas under isentropic conditions. Its chamber or nozzle entry velocity equals 70 m/sec, its final velocity 1500 m/sec. What is the change in enthalpy of the gas? What percentage of error is introduced if the initial velocity is neglected?
4. Nitrogen at  $500^\circ\text{C}$  ( $k = 1.38$ , molecular mass is 28.00) flows at a Mach number of 2.73. What are its actual and its acoustic velocity?

5. The following data are given for an optimum rocket:

Average molecular mass	24 kg/kg-mol
Chamber pressure	2.533 MPa
External pressure	0.090 MPa
Chamber temperature	2900 K
Throat area	0.00050 m <sup>2</sup>
Specific heat ratio	1.30

Determine (a) throat velocity; (b) specific volume at throat; (c) propellant flow and specific impulse; (d) thrust; (e) Mach number at throat.

6. Determine the ideal thrust coefficient for Problem 5 by two methods.
7. A certain ideal rocket with a nozzle area ratio of 2.3 and a throat area of 5 in.<sup>2</sup> delivers gases at  $k = 1.30$  and  $R = 66$  ft-lbf/lbm- $^\circ\text{R}$  at a design chamber pressure of 300 psia and a constant chamber temperature of 5300 R against a back pressure of 10 psia. By means of an appropriate valve arrangement, it is possible to throttle the propellant flow to the thrust chamber. Calculate and plot against pressure the following quantities for 300, 200, and 100 psia chamber pressure: (a) pressure ratio between chamber and atmosphere; (b) effective exhaust velocity for area ratio involved; (c) ideal exhaust velocity for optimum and actual area ratio; (d) propellant flow; (e) thrust; (f) specific impulse; (g) exit pressure; (h) exit temperature.
8. For an ideal rocket with a characteristic velocity  $c^* = 1500$  m/sec, a nozzle throat diameter of 18 cm, a thrust coefficient of 1.38, and a mass flow rate of 40 kg/sec, compute the chamber pressure, the thrust, and the specific impulse.
9. For the rocket unit given in Example 3–2 compute the exhaust velocity if the nozzle is cut off and the exit area is arbitrarily decreased by 50%. Estimate the losses in kinetic energy and thrust and express them as a percentage of the original kinetic energy and the original thrust.
10. What is the maximum velocity if the nozzle in Example 3–2 was designed to expand into a vacuum? If the expansion area ratio was 2000?

11. Construction of a variable-area nozzle has often been considered to make the operation of a rocket thrust chamber take place at the optimum expansion ratio at any altitude. Because of the enormous design difficulties of such a device, it has never been successfully realized. Assuming that such a mechanism can eventually be constructed, what would have to be the variation of the area ratio with altitude (plot up to 50 km) if such a rocket had a chamber pressure of 20 atm? Assume that  $k = 1.20$
12. Design a supersonic nozzle to operate at 10 km altitude with an area ratio of 8.0. For the hot gas take  $T_0 = 3000$  K,  $R = 378$  J/kg·K and  $k = 1.3$ . Determine the exit Mach number, exit velocity, and exit temperature, as well as the chamber pressure. If this chamber pressure is doubled, what happens to the thrust and the exit velocity? Assume no change in gas properties. How close to optimum nozzle expansion is this nozzle?
13. The German World War II A-4 propulsion system had a sea level thrust of 25,400 kg and a chamber pressure of 1.5 MPa. If the exit pressure is 0.084 MPa and the exit diameter 740 mm, what is the thrust at 25,000 m?
14. Derive Eq. 3-34. (*Hint:* Assume that all the mass flow originates at the apex of the cone.) Calculate the nozzle angle correction factor for a conical nozzle whose divergence half angle is  $13^\circ$ .
15. For Example 3-2, determine (a) the actual thrust; (b) the actual exhaust velocity; (c) the actual specific impulse; (d) the velocity correction factor. Assume that the thrust correction factor is 0.985 and the discharge correction factor is 1.050.
16. An ideal rocket has the following characteristics:

Chamber pressure	27.2 atm
Nozzle exit pressure	3 psia
Specific heat ratio	1.20
Average molecular mass	21.0 lbm/lb-mol
Chamber temperature	4200°F

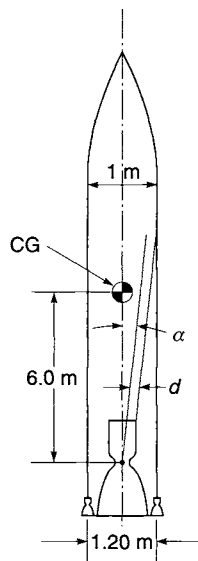
Determine the critical pressure ratio, the gas velocity at the throat, the expansion area ratio, and the theoretical nozzle exit velocity.

*Answers:* 0.5645; 3470 ft/sec; 14; and 8570 ft/sec.

17. For an ideal rocket with a characteristic velocity  $c^*$  of 1220 m/sec, a mass flow rate of 73.0 kg/sec, a thrust coefficient of 1.50, and a nozzle throat area of  $0.0248$  m<sup>2</sup>, compute the effective exhaust velocity, the thrust, the chamber pressure, and the specific impulse.

*Answers:* 1830 m/sec; 133,560 N;  $3.590 \times 10^6$  N/m<sup>2</sup>; 186.7 sec.

18. Derive equations 3-24 and 3-25.
19. A propulsion system with a thrust of 400,000 N is expected to have a maximum thrust misalignment  $\alpha$  of  $\pm 0.50$  degrees and a horizontal off-set  $d$  of the thrust vector of 0.125 in. as shown in this sketch. One of four small reaction control thrust chambers will be used to counteract the disturbing torque. What should be its maximum thrust level and best orientation? Distance of vernier gymbal to CG is 7 m.



## SYMBOLS

$A$	area, $\text{m}^2$ ( $\text{ft}^2$ )
$c$	effective exhaust velocity, $\text{m/sec}$ ( $\text{ft/sec}$ )
$c_p$	specific heat at constant pressure, $\text{J/kg-K}$ ( $\text{Btu/lbm-R}$ )
$c_s$	specific heat of solid, $\text{J/kg-K}$ ( $\text{Btu/lbm-R}$ )
$c_v$	specific heat at constant volume, $\text{J/kg-K}$ ( $\text{Btu/lbm-R}$ )
$c^*$	characteristic velocity, $\text{m/sec}$ ( $\text{ft/sec}$ )
$C_F$	thrust coefficient
$C_D$	discharge coefficient ( $1/c^*$ ), $\text{sec/m}$ ( $\text{sec/ft}$ )
$d$	total derivative
$D$	diameter, $\text{m}$ ( $\text{ft}$ )
$e$	energy conversion efficiency
$F$	thrust, $\text{N}$ ( $\text{lbf}$ )
$g_0$	standard sea level gravitational acceleration, $9.8066 \text{ m/sec}^2$ ( $32.174 \text{ ft/sec}^2$ )
$h$	enthalpy per unit mass, $\text{J/kg}$ ( $\text{Btu/lbm}$ )
$I_s$	specific impulse, $\text{sec}$ or $\text{N-sec}^3/\text{kg-m}$ ( $\text{lbf-sec/lbm}$ )
$J$	mechanical equivalent of heat; $J = 4.186 \text{ J/cal}$ in SI units or $1 \text{ Btu}$ $= 777.9 \text{ ft-lbf}$
$k$	specific heat ratio
$L$	length of nozzle, $\text{m}$ ( $\text{ft}$ )
$\dot{m}$	mass flow rate, $\text{kg/sec}$ ( $\text{lbm/sec}$ )
$M$	mach number
$\mathfrak{M}$	molecular mass, $\text{kg/kg-mol}$ (or molecular weight, $\text{lbm/lb-mol}$ )
$n_i$	molar fraction of species $i$
$p$	pressure, $\text{N/m}^2$ ( $\text{lbf/ft}^2$ or $\text{lbf/in.}^2$ )
$R$	gas constant per unit weight, $\text{J/kg-K}$ ( $\text{ft-lbf/lbm-R}$ ) ( $R = R'/\mathfrak{M}$ )
$R'$	universal gas constant, $8314.3 \text{ J/kg mol-K}$ ( $1544 \text{ ft-lb/lb mol-R}$ )
$T$	absolute temperature, $\text{K}$ ( $\text{R}$ )
$v$	velocity, $\text{m/sec}$ ( $\text{ft/sec}$ )
$V$	specific volume, $\text{m}^3/\text{kg}$ ( $\text{ft}^3/\text{lbm}$ )
$\dot{w}$	propellant weight flow rate, $\text{N/sec}$ ( $\text{lbf/sec}$ )

## Greek Letters

$\alpha$	half angle of divergent conical nozzle section
$\beta$	mass fraction of solid particles
$\epsilon$	area ratio $A_2/A_1$
$\zeta_d$	discharge correction factor
$\zeta_F$	thrust correction factor
$\zeta_v$	velocity correction factor
$\lambda$	divergence angle correction factor for conical nozzle exit

**Subscripts**

$a$	actual
$g$	gas
$i$	ideal, or a particular species in a mixture
max	maximum
opt	optimum nozzle expansion
$s$	solid
sep	point of separation
$t$	throat
$x$	any plane within rocket nozzle
$y$	any plane within rocket nozzle
0	stagnation or impact condition
1	nozzle inlet or chamber
2	nozzle exit
3	atmospheric or ambient

**REFERENCES**

- 3-1. A. H. Shapiro, *The Dynamics and Thermodynamics of Compressible Fluid Flow*, Vols. 1 and 2, The Ronald Press Company, New York, 1953 and M. J. Zucrow and J. D. Hoffman, *Gas Dynamics*, Vols. I and II, John Wiley & Sons, 1976 (has section on nozzle analysis by method of characteristics).
- 3-2. M. J. Moran and H. N. Shapiro, *Fundamentals of Engineering Thermodynamics*, Third edition, John Wiley & Sons, 1996; also additional text, 1997.
- 3-3. H. H. Koelle (Ed.), *Handbook of Astronautical Engineering*, McGraw-Hill Book Company, New York, 1961.
- 3-4. T. V. Nguyen and J. L. Pieper, "Nozzle Separation Prediction Techniques and Controlling Techniques," AIAA paper, 1996.
- 3-5. G. Hagemann, H. Immich, T. V. Nguyen, and D. E. Dumnov, "Advanced Rocket Nozzles," *Journal of Propulsion and Power*, Vol. 14, No. 5, pp. 620-634, AIAA, 1998.
- 3-6. M. Frey and G. Hagemann, "Flow Separation and Side-Loads in Rocket Nozzles," *AIAA Paper 99-2815*, June 1999.
- 3-7. G. P. Sutton, "Flow through a Combustion Zone," Section of Chapter 3, *Rocket Propulsion Elements*, John Wiley & Sons, Second, third, and fourth editions, 1956, 1963, and 1976.
- 3-8. J. A. Muss, T. V. Nguyen, E. J. Reske, and D. M. McDaniels, "Altitude Compensating Nozzle Concepts for RLV," *AIAA Paper 97-3222*, July 1997.
- 3-9. G. V. R. Rao, "Recent Developments in Rocket Nozzle Configurations," *ARS Journal*, Vol. 31, No. 11, November 1961, pp. 1488-1494; and G. V. R. Rao, "Exhaust Nozzle Contour for Optimum Thrust," *Jet Propulsion*, Vol. 28, June 1958, pp. 377-382.
- 3-10. J. M. Farley and C. E. Campbell, "Performance of Several Method-of-Characteristics Exhaust Nozzles," *NASA TN D-293*, October 1960.



- 3-11. J. D. Hoffman, "Design of Compressed Truncated Perfect Nozzles," *Journal of Propulsion and Power*, Vol. 3, No. 2, March-April 1987, pp. 150-156.
- 3-12. G. P. Sutton, *Stepped Nozzle*, U.S. Patent 5,779,151, 1998.
- 3-13. F. A. Williams, M. Barrère, and N. C. Huang, "Fundamental Aspects of Solid Propellant Rockets," *AGARDograph 116*, Advisory Group for Aerospace Research and Development, NATO, October 1969, 783 pages.
- 3-14. M. Barrère, A. Jaumotte, B. Fraeijs de Veubeke, and J. Vandenkerckhove, *Rocket Propulsion*, Elsevier Publishing Company, Amsterdam, 1960.
- 3-15. R. N. Knauber, "Thrust Misalignments of Fixed Nozzle Solid Rocket Motors," *AIAA Paper 92-2873*, 1992.
- 3-16. J. S. Lilley, "The Design and Optimization of Propulsion Systems Employing Scarfed Nozzles," *Journal of Spacecraft and Rockets*, Vol. 23, No. 6, November-December 1986, pp. 597-604; and J. S. Lilley, "Experimental Validation of a Performance Model for Scarfed Nozzles," *Journal of Spacecraft and Rockets*, Vol. 24, No. 5, September-October 1987, pp. 474-480.